



HAL
open science

Excited states of C₂H₄ studied by (3+1) and (3+2) REMPI spectroscopy: disentangling the lowest Rydberg series from the strong π - π^* $V \leftarrow N$ transition

Koutayba Alnama, Séverine Boyé-Péronne, Anne-Lise Roche, Dolores Gauyacq

► **To cite this version:**

Koutayba Alnama, Séverine Boyé-Péronne, Anne-Lise Roche, Dolores Gauyacq. Excited states of C₂H₄ studied by (3+1) and (3+2) REMPI spectroscopy: disentangling the lowest Rydberg series from the strong π - π^* $V \leftarrow N$ transition. *Molecular Physics*, 2007, 105 (11-12), pp.1743-1756. 10.1080/00268970701496524 . hal-00513117

HAL Id: hal-00513117

<https://hal.science/hal-00513117>

Submitted on 1 Sep 2010

HAL is a multi-disciplinary open access archive for the deposit and dissemination of scientific research documents, whether they are published or not. The documents may come from teaching and research institutions in France or abroad, or from public or private research centers.

L'archive ouverte pluridisciplinaire **HAL**, est destinée au dépôt et à la diffusion de documents scientifiques de niveau recherche, publiés ou non, émanant des établissements d'enseignement et de recherche français ou étrangers, des laboratoires publics ou privés.



Excited states of C₂H₄ studied by (3+1) and (3+2) REMPI spectroscopy: disentangling the lowest Rydberg series from the strong n-n* V←N transition

Journal:	<i>Molecular Physics</i>
Manuscript ID:	TMPH-2007-0068.R1
Manuscript Type:	Full Paper
Date Submitted by the Author:	01-Jun-2007
Complete List of Authors:	Alnama, Koutayba; Université Paris Sud, Laboratoire de PhotoPhysique Moléculaire Boyé-Péronne, Séverine; Université Paris Sud, Laboratoire de PhotoPhysique Moléculaire Roche, Anne-Lise; Université Paris Sud, Laboratoire de PhotoPhysique Moléculaire Gauyacq, Dolores; Université Paris Sud, Laboratoire de PhotoPhysique Moléculaire
Keywords:	ethylene, Rydberg states, REMPI spectroscopy, REMPI-PES



1
2
3
4
5 **Excited states of C₂H₄ studied by (3+1) and (3+2) REMPI**
6
7 **spectroscopy: disentangling the lowest Rydberg series**
8
9
10 **from the strong $\pi-\pi^*$ V←N transition**
11
12

13
14
15
16 **(Shortened version of the title: Three-photon REMPI spectra of C₂H₄)**
17
18
19
20

21
22 K. ALNAMA^{a),b)}, S. BOYÉ-PÉRONNE^{a)}, A.-L. ROCHE^{a)}, and D. GAUYACQ^{*a)}
23
24

25
26
27 a) Laboratoire de Photophysique Moléculaire, CNRS UPR 3361, Bât. 210,
28

29
30 Université Paris-Sud, 91405 Orsay Cédex, France

31
32 b) Permanent address: Atomic Energy Commission of Syria, P.O. BOX 6091, Damascus, Syria
33
34

35
36
37 *Corresponding author. Telephone: (+33) 1 69156307; Fax: (+33) 1 69156777; E-mail:
38

39 dolores.gauyacq@ppm.u-psud.fr
40
41
42
43
44
45
46
47
48
49
50
51
52
53
54
55
56
57
58
59
60

1
2 (3+1) and (3+2) Resonantly Enhanced Multiphoton (REMPI) spectroscopy has been
3
4 carried out to study the Rydberg states of C₂H₄ in the region 55000-83000 cm⁻¹.
5
6 Differences and similarities were observed between these three-photon spectra and the
7
8 one-photon absorption spectrum. First, the disappearance of the strong $\pi\text{-}\pi^*$ V \leftarrow N
9
10 valence transition from the REMPI spectra allowed to disentangle the vibrational
11
12 structure of the 3s Rydberg transition from the V \leftarrow N quasi-continuum, and to search for
13
14 additional weak transitions. Earlier vibrational assignments from the absorption
15
16 spectrum have been confirmed in the REMPI analysis of the 3s \leftarrow N and ns,nd \leftarrow N
17
18 transition systems, although with very different band intensities. This analysis has
19
20 provided additional weak band assignments involving the ν_3 mode in the observed
21
22 Rydberg transitions. New electronic components (3d π_y , 4d π_y , 5d π_y) of the nd complex
23
24 which are three-photon allowed but one-photon forbidden, have been tentatively
25
26 assigned. The photoelectron (PES) spectra of the 3s and 3d σ lowest vibrational levels
27
28 have revealed a deviation from a pure Rydberg character, in apparent contradiction with
29
30 previous (2+1) REMPI-PES data involving *gerade* vibronic levels of the 3s Rydberg
31
32 state, which led to a prominent Rydberg character for this state. Rydberg-valence and
33
34 Rydberg-Rydberg vibronic interactions mediated via non-symmetric modes could
35
36 explain the different behaviour between *gerade* and *ungerade* vibronic levels of the
37
38 ethylene Rydberg states.
39
40
41
42
43
44
45
46
47
48
49
50
51
52
53
54
55
56
57
58
59
60

Keywords: ethylene; Rydberg states; REMPI spectroscopy; REMPI-PES

1. INTRODUCTION

Although the ethylene molecule is of fundamental interest both for organic photochemistry and for electronic structure theory, our understanding of the spectroscopy of this molecule is far from complete [1],[2,3]. Despite decades of spectroscopic investigations and electronic structure calculations, many questions remain unanswered concerning the assignment of the vacuum-ultraviolet (VUV) spectrum of ethylene. Indeed the absorption spectrum exhibits severe overlapping of valence-valence and Rydberg-valence transitions with the appearance of many diffuse vibrational bands. According to Mulliken's notations [4], the ground state and lowest valence excited states are designed as N (for normal), V (for the $\pi\pi^*$ Valence) and Z (for the π^{*2} Zwitterionic), while the lowest Rydberg state, the 3s state, is designed as R. The $\pi-\pi^*$, $V^1B_{1u} \leftarrow N^1A_g$ transition exhibits an extremely extended quasi-continuum, with a broad vibrational structure which has been the subject of many questions, including the effect of Duschinsky rotation and the effect of the large amplitude torsional mode [5],[6],[7],[8],[9],[10],[11]. Recently, new dynamic information has been obtained by femtosecond pump-probe spectroscopy in the region around 6 eV [12],[13]. The lifetime of the $\pi\pi^*$ V state has been determined as 30 ± 15 fs [12] and 20 ± 10 fs [13], in agreement with the broad vibrational bands, showing a typical bandwidth of about 400 cm^{-1} .

Concerning the absorption transitions towards Rydberg states, the electronic origin bands of the *ns* and *nd* states and their vibrational progressions have been observed with sharper profiles than those of the $V \leftarrow N$ transition, although they all present some spectral broadening. The analysis of the ethylene Rydberg transitions, as compared for instance to linear acetylene, has been proved non trivial due to the large geometry change between the ground state, the Rydberg states and the cationic ground state. The most complete vibrational analysis of the *ns* and *nd* Rydberg transitions

1 including partially or totally deuterated isotopomers has been performed by McDiarmid
2 [14]. This analysis allowed unambiguous assignments of several ns and nd band origins
3
4
5
6 from $n=3$ to 6. Nevertheless, some absorption features remained unexplained or
7
8 tentatively assigned. Table 1 recalls the definition of the twelve normal modes of
9
10 ethylene with the symmetry conventions adopted in the present paper. The most active
11
12 bands in the Rydberg absorption transitions involve the ν_4 torsion mode and the ν_2 CC
13
14 stretching mode. In addition, bands involving the ν_3 CH₂ scissors mode have also been
15
16 observed, though with a weaker intensity.
17
18
19

20
21 [insert table 1 about here]
22

23
24 Rydberg-valence interactions in ethylene have been the subject of many
25
26 theoretical investigations [15],[16],[17],[18],[19],[20],[21],[22],[23],[24]. Indeed, the
27
28 observation of Rydberg transitions in the same region as the $V\ ^1B_{1u} \leftarrow N\ ^1A_g$ transition
29
30 opened a question about a valence-Rydberg interaction through vibronic coupling,
31
32 already addressed in the earlier work of Wilkinson and Mulliken [5]. Buenker and
33
34 Peyerimhoff [15] found a Rydberg-valence mixing between the $V\ ^1B_{1u}$ state and the
35
36 $3d\pi_x\ ^1B_{1u}$ state calculated by *ab initio* approaches, which was the beginning of a
37
38 longstanding controversy on the Rydberg character of the V state: Mulliken discussed in
39
40 detail this point, by considering the concept of core molecular orbital precursors for
41
42 describing the Rydberg molecular orbitals, and rejected the existence of two separate V
43
44 and $3d\pi_x$ states [16]. In the case of NO, Jungen [25] has discussed a similar situation
45
46 through a very insightful paper which clearly highlights Mulliken's concept of precursor
47
48 in Rydberg orbitals. The ethylene controversy was summarized later on by Wiberg *et al.*
49
50 [17] who, again by considering Mulliken's precursor definition, reconciled the point of
51
52 view of Buenker and Peyerimhoff [15] and that of Mulliken [16]. Petrongolo *et al.*
53
54 [18],[19] calculated another important nonadiabatic coupling between the $V\ ^1B_{1u}$ state
55
56 and the $3p_y\ ^1B_{1g}$ Rydberg state, via the torsional coordinate of a_u symmetry. Later on,
57
58
59
60

1 Siebrand *et al.* [20] proposed a vibronic coupling between the V $^1B_{1u}$ state and the
2 lowest $3s$ $^1B_{3u}$ Rydberg state via the ν_7 wagging mode (b_{2g} symmetry as defined in
3 Table 1). More recently, this vibronic coupling has been reinvestigated by Mebel *et al.*
4 [21], who found, in addition, a significant intra-Rydberg vibronic coupling between the
5 $3p_y$ and the $3s$ states via the ν_8 and ν_9 modes (with the definition of Table 1).
6 Interestingly, these authors also studied the internal conversion both from the $\pi\pi^*$ V
7 state and from the $3s$ state towards the ground state.
8

9
10
11
12
13
14
15
16
17
18
19 Very accurate *ab initio* calculations have been performed on the low lying
20 Rydberg states embedded in the valence V state of C_2H_4 , in particular in the vertical
21 excitation region from the planar ground state zero energy up to 8 eV
22 [7],[9],[21],[22],[23],[24]. In some of these latter studies [21],[22],[23],[24], several
23 conical intersections connecting the V state to low lying Rydberg states have been
24 identified, yet without providing further details on Rydberg-valence interactions.
25

26
27
28
29
30
31
32
33 The present work focuses on the Rydberg state analysis via three-photon
34 excitation, multiphoton ionisation. Resonantly-enhanced multiphoton ionisation
35 (REMPI) and photoelectron spectroscopy (REMPI-PES) spectra have been proved very
36 efficient for extracting information on the Rydberg character and the Rydberg-valence
37 interaction (see for instance Ref. [26] in the case of acetylene). Surprisingly, very few
38 REMPI studies have been performed on ethylene, except for two-photon excitation
39 studies, which have revealed the structure of the gerade np and nf states [27],[28],[29].
40 In one of these two-photon studies, vibronic bands involving odd quanta of ν_4 for the $3s$
41 Rydberg state have also been observed [29].
42

43
44
45
46
47
48
49
50
51
52
53
54
55 To our knowledge, no three-photon REMPI spectra of ethylene have been
56 reported yet in the literature. These three-photon spectra bring pieces of information
57 complementary to the absorption spectrum:
58
59
60

- 1
2
3
4
5
6
7
8
9
10
11
12
13
14
15
16
17
18
19
20
21
22
23
24
25
26
27
- i) The REMPI technique strongly favours observation of the Rydberg states with respect to excited valence states: indeed, the Rydberg electron is easily ionised by the last photon, and moreover, very unstable valence states decay much faster than they ionise, and cannot be observed by ionisation with the typical laser power density used in REMPI spectroscopy.
 - ii) The three-photon spectra almost share the same selection rules with the one-photon absorption spectrum (odd number of photons). Hence observation of the ns and nd Rydberg states is strongly allowed and can shed light on some questionable assignments of the absorption spectrum. Moreover, additional symmetry-allowed transitions can be observed, such as A_u vibronic levels.

28
29
30
31
32
33
34
35
36
37
38
39
40
41

This paper presents a detailed vibrational analysis of the observed (3+1) and (3+2) REMPI spectra of C_2H_4 in the 55000-83000 cm^{-1} three-photon energy region. REMPI-PES spectra have also been recorded from resonant $3s$ and $3d$ vibronic levels and are discussed with respect to the Rydberg character of these low-lying Rydberg states, as well as in the context of possible Rydberg-valence interactions.

42 2. EXPERIMENTAL

43
44
45
46
47
48
49
50
51
52
53
54
55
56
57
58
59
60

The (3+1) and (3+2) REMPI experiments were performed in a magnetic bottle electron spectrometer, described elsewhere [30]. Ethylene was introduced into a vacuum chamber through a 2-mm diameter hole. The typical background pressure was 8.10^{-5} mbar in the interaction region, so that an effusive beam condition allowed for moderate rotational cooling of the molecules (170K-typical rotational temperature). Tuneable radiation was generated by an excimer (XeCl, LUMONICS PM 886) pumped dye laser (Lambda Physik FL2002) operating with different dye solutions covering the spectral region 538-360 nm (coumarin 500, coumarin 480, coumarin 460, coumarin 440, furan

1, PBBO and QUI), with a typical bandwidth of 0.3 cm^{-1} for one-photon energy. The laser beam was focused with a 150 mm focal length lens. The laser energy at the entrance of the magnetic bottle varied between 3 mJ and 7 mJ per pulse for the spectral region corresponding to a (3+1) photon ionisation process, depending on the dye solution. For the (3+2) photon ionisation process, energies between 5 and 10 mJ per pulse were used. The laser was operating at 10 Hz with a typical pulse duration of 10 ns. Two different spectra were recorded:

(i) The total photoelectron signal was collected as a function of the laser wavelength by a microchannel plate detection system. An appropriate time-gate selected the electrons produced by the (3+1) or (3+2) ionisation process in ethylene, and the signal was accumulated over about 10 laser shots. The photon wavelength was calibrated in the $55000\text{-}83000 \text{ cm}^{-1}$ three-photon energy region by recording the optogalvanic spectrum of an iron-neon hollow cathode [31]. It should be noted that many spectral features present quite broad linewidths. Although the absolute accuracy of the quoted energies is $\pm 1 \text{ cm}^{-1}$, the broadening of the observed bands and the strong overlap in these regions lead to an estimated precision on the vibrational band positions of $\pm 20 \text{ cm}^{-1}$.

(ii) Time-of-flight photoelectron spectra were recorded at fixed three-photon wavelengths. Careful energy calibration of these PES spectra was performed by constructing a calibration curve from the (3+1) REMPI-PES signal via the $3d\sigma$ origin band of ethylene recorded at different retarding bias voltages V_g . The calibration was performed following the law:

$$E_{kin} = \left(\frac{A}{t_{TOF} - t_0} \right)^2 - V_0 - V_g \quad (1)$$

where E_{kin} is the kinetic energy of the photoelectrons in eV, t_{TOF} is their arrival time at the detector in nanoseconds, t_0 (in ns) and V_0 (in V) are time and voltage parameters,

1
2 and A is a geometrical parameter of the magnetic bottle ($A = 844 \text{ eV}^{1/2} \cdot \text{ns}$). The best
3
4 PES spectra have been obtained by accumulating the signal over 3000 laser shots, and
5
6 by applying a moderate retarding bias voltage, between -0.06 V and -0.4 V , insuring a
7
8 compromise between electron energy resolution (around 90 meV at low kinetic energy)
9
10 and photoelectron signal detection threshold.
11
12

13
14
15 For comparison with the present REMPI spectra, the one-photon VUV
16
17 absorption spectrum of C_2H_4 has been recorded over the same excitation range at the
18
19 synchrotron radiation facility in Orsay (Super-ACO) on the SA63 beam line. The SA63
20
21 beam line was equipped with a 3-m Eagle normal incidence monochromator and a 1800
22
23 grooves/mm grating tuned in the 188-112 nm spectral region with a 0.08 nm resolution
24
25 (i.e. $60\text{-}70 \text{ cm}^{-1}$). In the experiment performed with this beamline, ethylene was
26
27 introduced into a vacuum chamber by means of a stainless steel needle with a $100\text{-}\mu\text{m}$
28
29 internal diameter, and excited by the VUV beam. A background pressure of about 10^{-4}
30
31 mbar was maintained in the vacuum chamber. The transmitted VUV light was recorded
32
33 through the visible fluorescence of a coated sodium salicylate window and collected by
34
35 a photomultiplier tube (Hamamatsu R928, spectral range $950\text{-}185 \text{ nm}$).
36
37
38
39
40
41
42
43
44

45 3. RESULTS AND DISCUSSION

46 3.1. Brief summary on the selection rules in REMPI spectra

47
48 As was pointed out by Willitsch *et al.* [32], in the case of the twisted cation ground state
49
50 of ethylene, the adequate molecular symmetry group remains D_{2h} . The same symmetry
51
52 prescription holds for all Rydberg states of neutral ethylene converging to the cation
53
54 ground state, for which the robust g/u symmetry has been noticed to govern the whole
55
56 absorption spectrum [14]. Therefore, the REMPI spectroscopy can be divided in two
57
58
59
60

1
2 groups of experiments depending on the number of photons involved in the excitation
3
4 step.

5
6
7 (i) *one-photon and three-photon excitation*: From the neutral ground state 1A_g , only
8
9 vibronic levels of $^1B_{1u}$, $^1B_{2u}$ and $^1B_{3u}$ are accessible in one-photon. In addition,
10
11 vibronic levels 1A_u symmetry are also accessible by three-photon excitation. This is
12
13 why the present (3+2) and (3+1) spectra are dominated by the same vibronic
14
15 structure as the absorption spectrum, as will be shown in the following sections.

16
17
18 (ii) *two-photon and four-photon excitation*: From the neutral ground state 1A_g , only
19
20 vibronic levels of 1A_g , $^1B_{1g}$, $^1B_{2g}$ and $^1B_{3g}$, are accessible in two- and four-photon
21
22 experiments. This is the case of the (2+1) photon REMPI work of Ref. [29] and of
23
24 the (4+1) photon weak bands observed in the present work and discussed in section
25
26 3.3.2 below.
27
28
29

30 31 32 **3.2. Overview of the three-photon excitation spectrum of ethylene**

33
34
35 Figure 1 presents an overview of the three-photon spectra of ethylene, together with its
36
37 corresponding one-photon absorption spectrum, in the $55000\text{-}83000\text{ cm}^{-1}$ three-photon
38
39 energy region. The three-photon spectra have been obtained with seven different dye
40
41 laser solutions and could not be normalised to each other because of poor overlapping
42
43 transitions in the different overlapping dye spectral regions. Inside each spectral region,
44
45 a drastic dependence upon laser intensity is expected and can affect the three-photon
46
47 REMPI intensity spectra, but this dependence has not been studied systematically.
48
49 Consequently, the spectra of Fig.1b have not been corrected from laser intensity and the
50
51 dye laser intensity curves have been added in Fig.1c. Note that in the low energy region
52
53 (i.e. below 63593 cm^{-1}), the ionisation step requires two photons, as shown in Fig. 1.
54
55
56
57
58

59 [insert Figure 1 about here]
60

1
2 If one considers first the one-photon absorption spectrum, the explored spectral
3 range can be divided into two main regions: The low energy range (55000-68000 cm^{-1})
4 exhibits the very strong $V \leftarrow N$ bands superimposed by the sharper vibrational structure
5 of the lowest $3s$ transition. Above 68000 cm^{-1} , the ns and nd Rydberg series show up
6 with more or less diffuse vibrational structures from the $3d\sigma$ origin at 69530 cm^{-1} .
7 Following the pioneering work of Wilkinson and Mulliken [5], this absorption spectrum
8 has been analysed in details by Merer and Schoonveld [33] in the $3s$ transition region,
9 and by McDiarmid [14] for the ns and nd series.
10
11
12
13
14
15
16
17
18
19
20

21 Let us now consider the three-photon REMPI spectra. A very different aspect is
22 observed between the three-photon and the absorption spectra, both in structure and
23 relative intensity, unlike the case of acetylene [34]. In particular, two striking features
24 appear in Fig. 1 by comparison with the one-photon absorption spectrum:
25
26
27
28
29

30 (i) In the 55000-64000 cm^{-1} three-photon energy region, the $V \leftarrow N$ transition is
31 completely absent from the REMPI spectrum. This allows to completely disentangle the
32 vibronic structure of the $3s$ Rydberg state from the underlying $V \leftarrow N$ strong quasi-
33 continuum, and to search for new weaker transitions. Section 3.3 below is devoted to
34 the analysis of these $3s$ vibrational bands.
35
36
37
38
39
40
41

42 (ii) In the 68000-83000 cm^{-1} three-photon energy region, both Rydberg structures
43 and vibrational bands of ns and nd Rydberg states notably differ from the absorption
44 spectrum, making the assignment of the REMPI spectra very difficult at first sight.
45 Some strong features in the absorption spectrum, as the $4d\delta$ origin band at 77604 cm^{-1} ,
46 almost disappear in the REMPI spectra. This is most probably indicative of large
47 variations in the decay dynamics of the Rydberg components in this region, as discussed
48 in section 3.4.
49
50
51
52
53
54
55
56
57
58
59
60

3.3. The $3s$ Rydberg transition studied via (3+2) photon ionisation

The $3s$ absorption spectrum has been analysed in detail by Merer and collaborators [35],[33] who established from their analysis the twisted equilibrium geometry of the $3s$ Rydberg state. These authors derived a value for the torsion angle of 25° , and a value for the inversion barrier to planarity of about 290 cm^{-1} . This twisted geometry is very similar to the one established more recently for the ground state of the C_2H_4^+ cation, i.e. 29° torsion angle (see Ref. [32] and Table VI therein). Later on, the geometry of the $3s$ state was reconsidered by Foo and Innes [36], who proposed a different evaluation of the torsion angle of 37° , from the spectral analysis of the $3s$ absorption spectrum in different isotopomers of ethylene. However, this latter value seems overestimated by comparison with the recently measured cation value [32], and also by comparison with recent *ab initio* calculations [7]. The change in the equilibrium torsional angle of the $3s$ state with respect to the planar ground state is responsible for an activity in the ν_4 torsional mode (a_u) which had been noticed already in the first absorption analysis by Wilkinson and Mulliken [5].

Table 1 presents the different normal modes of ethylene, together with their corresponding frequencies, in the neutral ground state, in the $3s$ state and in the cation ground state. Both the D_2 and D_{2h} symmetry labels are reported in this table for the different modes. As pointed out in paragraph 3.1 above, D_{2h} symmetry group is pertinent for transitions towards Rydberg states from the neutral ground state, and it rules out excitation of odd quanta of ν_4 in the Rydberg states. The corresponding vibrational levels do not appear indeed in the REMPI spectra as shown below.

[insert table 2 about here]

Table 2 recalls the calculated geometrical parameters of the $3s$ state as compared with the neutral ground state and the cation ground state. Upon excitation of the π ($1b_{3u}$) valence orbital to the $3s$ Rydberg orbital, a lengthening of the C=C bond occurs from

1
2 the ground state to the $3s$ state [7], in good agreement with the experimental value [33].
3
4 In the cation, the C=C bond length has been calculated [37] to 1.4004 Å, close to that of
5
6 the $3s$ state. Excitation of the π orbital to the $3s$ orbital results in a twisted geometry as
7
8 said above. As shown in Table 2 the equilibrium torsion angles are very close in the $3s$
9
10 state [7] and in the cation ground state [37]. On what concerns the HCH scissor angle, it
11
12 is larger in the $3s$ Rydberg state than in the neutral ground state, and even larger than in
13
14 the cation ground state. From these values (see Table 2), the expected main contribution
15
16 to the REMPI spectrum should consist of excitation to totally symmetric vibronic levels
17
18 of the $3s$ state involving even quanta of the ν_4 torsion mode, and progressions in the ν_2
19
20 CC stretching mode and finally in the ν_3 CH₂ scissor mode.
21
22
23
24
25
26
27

28 3.3.1. Vibrational assignment

29
30 [insert figure 2 about here]

31
32
33 Figure 2 displays the (3+2) photon REMPI spectrum in the region of the $3s$ state. As
34
35 expected from the very short lifetime of the $\pi\pi^*$ V state, the observed features in the
36
37 energy range covered by Fig. 2 belong exclusively to the Rydberg transitions. Like in
38
39 the absorption spectrum [33] and as expected from the geometry changes described
40
41 above, the vibrational structure is dominated by progressions in $m\nu_2$ and $m\nu_2+2\nu_4$, but
42
43 surprisingly not by ν_3 bands. Note that the intensity of the vibrational transitions of Fig.
44
45 2 has not been corrected by the laser dye intensity. It is remarkable though that the
46
47 relative vibrational intensities and bandwidths match very well those of the absorption
48
49 spectrum, as shown in Fig. 1.
50
51
52
53

54
55 As was proposed earlier by Wilkinson and Mulliken [5] (see also page 534 of Ref.
56
57 [38]), and by Merer and Schoonveld [35], from the absorption spectrum analysis, a
58
59 progression in $m\nu_2+4\nu_4$ appears in the REMPI spectra as barely resolved shoulders lying
60
on the red side of the $(m+1)\nu_2$ bands. Our determination of $4\nu_4$ reported in Table 1 is in

1
2 good agreement with the value proposed by Ref. [35]. Table 3 summarizes all the
3
4 present three-photon assignments.
5

6
7 [insert table 3 about here]
8

9 At this point, it is interesting to take advantage of the absence of the underlying
10 V-N broad bands, for searching much weaker vibrational transitions in the $3s$ (3+2)
11 REMPI spectrum. In particular, the observation of the ν_3 CH₂ scissor vibration has been
12 recently proposed in the (2+1) REMPI spectrum of C₂H₄ by Rijkenberg and Buma [29]
13 through the observation of a two-photon symmetry allowed combination band $\nu_4+\nu_3$
14 leading to an estimated value of ν_3 of 1146 cm⁻¹ for C₂H₄. The search for three-photon
15 allowed bands involving the ν_3 mode in our spectrum results in a possible $m\nu_2+\nu_3$
16 progression shown in the spectrum of Fig. 2 with a ν_3 frequency value, given in Table 1,
17 close to the value proposed from the two-photon spectrum [29]. Unfortunately, these
18 bands are almost completely overlapped by the $m\nu_2+4\nu_4$ bands, which makes the ν_3
19 assignment only tentative at this stage of the analysis.
20
21
22
23
24
25
26
27
28
29
30
31
32
33
34

35
36 A more detailed comparison between our (3+2) REMPI data and the (2+1)
37 REMPI data obtained by Rijkenberg and Buma [29] on the $3s$ state, reveals a
38 discrepancy between the ν_2 frequency derived from their two-photon spectra analysis
39 and the ν_2 frequency measured either in the present (3+2) REMPI spectrum or in the
40 one-photon absorption spectrum [14]: from the assignment of the $\nu_2+\nu_4$ combination
41 band, Rijkenberg and Buma [29] extracted a ν_2 frequency of 1525 cm⁻¹, by far too large
42 as compared to the previous value of 1380 cm⁻¹ found by Wilkinson and Mulliken [5],
43 or by McDiarmid [14], or by the present work. This discrepancy can be corrected by
44 proposing two re-assignments of the (2+1) REMPI spectra of C₂H₄ and C₂D₄ in Ref.
45 [29]:
46
47
48
49
50
51
52
53
54
55
56
57
58
59
60

The first one consists of exchanging the assignments of the $\nu_2+\nu_4$ band and $5\nu_4$
band in C₂H₄. One convincing argument for exchanging these assignments is the

1
2 comparison between the vibrational spacing observed in the (2+1) REMPI-PES spectra
3 of Ref. [29], recorded from the above cited two-photon bands, and the corresponding
4 spacing measured with a better accuracy in the ZEKE spectrum of Ref. [32]. This
5 reassignment of the (2+1) photon spectra leads to a ν_2 value in the $3s$ state of C_2H_4 of
6 1336 cm^{-1} , and to a ν_2^+ value in the ground state of the $C_2H_4^+$ cation of 1480 cm^{-1} , in
7 better agreement with the previously measured $3s$ frequency [33], and with the more
8 recent cation frequency [32], respectively.

9
10 The above re-assignment of the two-photon bands in C_2H_4 implies a second re-
11 assignment of the $3s$ two-photon bands of C_2D_4 in Ref. [29], in order to keep a
12 consistent isotopic ratio between the C_2H_4 and C_2D_4 mode frequencies for the $5\nu_4$
13 bands. This can be done by exchanging the assignments of the $\nu_3+\nu_4$ and $5\nu_4$ bands in
14 the two-photon spectrum of C_2D_4 , in Ref. [29]. Again, these new assignment in C_2D_4
15 brings vibrational spacings in the cation, measured from the corresponding PES spectra
16 of Ref. [29], i.e. $5\nu_4^+ \approx 1000\text{ cm}^{-1}$ in better agreement with the ZEKE values of Ref.
17 [32], that is 982 cm^{-1} . In addition, these new assignments reasonably match the expected
18 isotopic ratio for the ν_3 frequency in the $3s$ state (i.e. 0.76).

3.3.2 Occurrence of (4+1) REMPI features embedded in the (3+2) REMPI spectra

19
20 Apart from the tentatively assigned combination bands involving ν_3 , other weaker
21 structures appear in Fig. 2. Some of these observed structures are reminiscent of (4+1)
22 REMPI nf transitions. The assignments proposed in Table 3, and displayed in Figure 2,
23 are supported by the previous observation of nf Rydberg states in the (2+1) photon
24 REMPI spectra of C_2H_4 and C_2D_4 [28]. Indeed, possible (4+1) resonances, reported in
25 Table 3, may occur superimposed on the (3+2) REMPI spectrum. Therefore an energy
26 scale for the four-photon energy is given at the top of Figure 2 and corresponds to the
27 region of the $4f$ and $5f$ complexes. The nf complexes have been analysed via two-photon
28
29
30
31
32
33
34
35
36
37
38
39
40
41
42
43
44
45
46
47
48
49
50
51
52
53
54
55
56
57
58
59
60

1 spectroscopy by Williams and Cool [28] ($n=7-13$ for C_2H_4 and $n=4-17$ for C_2D_4). They
2 essentially consist of two electronic components named by these authors as f_I and f_{II} ,
3 and exhibit mainly excitation in $2\nu_4$. The observed positions in Figure 2 match very well
4 the expected positions in C_2H_4 derived by applying the pertinent isotopic shift for origin
5 bands and excited vibrational bands, extracted from Ref. [28].
6
7
8
9
10
11
12

13
14 The non penetrating nf states are expected to be unperturbed and to mimic the
15 ionic ground state vibrational structure. The $2\nu_4$ and ν_2 frequencies derived from the
16 present (4+1) photon analysis of Table 3 are in agreement with the frequencies
17 previously derived from the two-photon analysis, and are very close indeed to the ion
18 frequencies given by Willitsch *et al.* [32]. More importantly, the observation of the very
19 weak nf transitions demonstrates that the REMPI spectrum displayed in Fig. 2 is, by far,
20 dominated by (3+2) processes in the $57000-63000\text{ cm}^{-1}$ region. Four-photon resonances
21 remain a minor process in this region and therefore should not contaminate the
22 photoelectron spectra recorded in the same region and shown in paragraph 3.3.4.
23
24
25
26
27
28
29
30
31
32
33
34

35 Another point concerns the weak feature at 79515 cm^{-1} (four-photon energy): it
36 is assigned to the $4f_I\ 3^1\ 4^2$ band by assuming a $\nu_3+2\nu_4$ band frequency identical to that
37 of the cation [32]. Note that in the C_2D_4 isotopomer, this vibrational band has also been
38 observed for the $4f_I$ state [28]. The ν_3 frequency of the $4f$ Rydberg states is very close to
39 that of the cation ground state, and finally is also in agreement with the two-photon
40 assignment of Ref. [28].
41
42
43
44
45
46
47
48
49
50
51
52

53 3.3.3 Summary on the ν_2 vibration frequency of the $3s$ state

54 It is interesting to compare the vibrational band intensities in the $3s$ transitions with that
55 of the PES spectrum recorded by Holland *et al.* [39]. This photoelectron spectrum
56 shows weaker ν_2 progressions as compared to strong ν_3 progressions. These intensities
57 have been explained by a Duschinsky rotation occurring in the transition from the
58
59
60

1
2 neutral ground state to the cation ground state, favouring the observation of ν_3 with
3
4 respect to ν_2 . Note that the corresponding PES spectrum [39] of C_2D_4 shows on the
5
6 other hand a dominant intensity of the ν_2 progressions as compared to the ν_3 bands,
7
8 corresponding to a different Duschinsky matrix in this isotopomer. The PFI-ZEKE
9
10 spectrum of Willitsch *et al.* [32] exhibits with very high rotational resolution a similar
11
12 trend favouring the ν_3 and $\nu_3+2\nu_4$ bands with respect to the ν_2 and $\nu_2+2\nu_4$ bands in
13
14 $C_2H_4^+$, and the reverse trend for $C_2D_4^+$. This situation has already been confirmed by
15
16 Rijkenberg and Buma [29] who calculated the Franck-Condon factors and Duschinsky
17
18 matrix upon ionisation of C_2H_4 and C_2D_4 . Excitation from the neutral ground state to the
19
20 $3s$ state shows very weak Franck-Condon factors involving the ν_3 scissor mode in our
21
22 REMPI spectra as well as in the absorption spectrum, indicating a different situation as
23
24 compared to excitation towards the cation ground state. Given the similar geometries
25
26 between the $3s$ state and the cation ground state (see Table 2), these Franck-Condon
27
28 factors are still unexplained.
29
30
31
32
33
34

35
36 A general comment can be drawn by comparing the measured vibrational
37
38 frequencies reported in Table 1. As expected from a Rydberg state, the observed $3s$
39
40 frequencies are much closer to the cation ground state frequencies than to the neutral
41
42 ground state value. Nevertheless, the ν_2 CC stretching frequency is significantly lower
43
44 in the $3s$ state than in the cation ground state, which is rather surprising given the almost
45
46 equal CC bond lengths in both states (see Table 2). This intriguing point has never been
47
48 commented to our knowledge, neither by spectroscopists nor by theoreticians. One
49
50 would expect the CC bond to be weaker in the cation than in the $3s$ Rydberg state.
51
52 Indeed, this lowest Rydberg orbital is expected to be rather penetrating and to
53
54 participate to some extent to the stability of the molecule. If the lower ν_2 frequency
55
56 value is to be correlated with a weakening of the CC bond in the $3s$ state (although this
57
58 correlation does not seem to be obvious from the computed equilibrium geometries of
59
60

1
2 Table 2), it could therefore reveal a slightly antibonding character of the $3s$ orbital. This
3
4 would deserve a more thorough analysis in terms of computed molecular orbitals.
5
6
7

8 9 3.3.4 Rydberg character of the $3s$ state: Photoelectron spectra

10
11 [insert Figure 3 about here]
12

13
14 The deviation from the Rydberg character of the $3s$ state can be better analysed through
15 the PES spectra. Three (3+2) REMPI-PES spectra have been recorded in the $3s$ region
16 and are presented in Figure 3. They correspond to ionisation from the $3s$ origin (panel
17 a), from the $3s4^2$ level (panel b) and from the $3s2^1$ level (panel c). Although the
18 vibrational structure of the cation is barely resolved, assignments are still possible from
19 these spectra. The strongest peaks around the zero ion internal energy correspond to the
20 expected $\Delta v_i=0$ propensity rule for a Rydberg state. In addition, significant ionisation to
21 mv_2^+ , v_3^+ and $mv_2^++2v_4^+$ also occurs, indicating a deviation from a pure Rydberg
22 character. The PES signal deteriorates with increasing energy; hence no assignment was
23 attempted for the highest energy features in Figs (3b) and (3c). The peaks around the
24 zero ion internal energy are expected to show a comparable resolution in the three
25 panels of Fig. 3. Thus, the increasing broadening from panel (a) to panel (c) has been
26 interpreted as unresolved and overlapping vibrational peaks, tentatively assigned in Figs
27 3 by reporting the accurate cation frequencies of Ref. [32] in dashed lines. The observed
28 vibrational activity in the PES spectrum can be understood in terms of non pure
29 Rydberg state, which is rather common for the lowest $3s$ Rydberg state of such
30 molecules. If one now compares the present PES spectra with those obtained by
31 Rijkenberg and Buma [29] in the (2+1) ionisation via the $3s4^3$ level, with a much better
32 resolution in their case, a striking difference is observed: in Ref. [29], only one
33 prominent photoelectron peak shows up at the $3v_4^+$ frequency of the ion, so that the
34 authors concluded to a predominant Rydberg character for the $3s$ Rydberg state of

35
36
37
38
39
40
41
42
43
44
45
46
47
48
49
50
51
52
53
54
55
56
57
58
59
60

1
2 ethylene. Two reasons can be proposed to explain this very surprising different
3
4 behaviour of the 3s state in our PES spectra:
5

6
7 - our (3+2) REMPI-PES spectrum may be contaminated by a quasi resonant state at the
8
9 fourth photon energy: this hypothesis is very unlikely, since we have shown in section
10
11 3.3.2 that the $4f$ and $5f$ states lying at the four-photon energy bring a very weak
12
13 contribution to the REMPI spectrum of Figure 2, and therefore should not contribute to
14
15 strong features in the PES spectrum.
16
17

18
19 - the (2+1) REMPI-PES experiment of Ref. [29] probes vibronic intermediate levels of
20
21 *gerade* symmetry in the D_{2h} group, while our experiment probes *ungerade* vibronic
22
23 intermediate levels, as said in section 3.1. Thus everything behaves as if the 3s
24
25 vibrational levels of *g* symmetry conformed to an almost pure Rydberg character, while
26
27 those of *u* symmetry (including the vibrationless level) behaved as less pure Rydberg
28
29 levels. A Rydberg-valence or a Rydberg-Rydberg vibronic coupling mediated by one
30
31 active mode might be invoked, as in the theoretical work of Mebel *et al.* [21]. For
32
33 instance these authors calculated a weak vibronic coupling between the 3s Rydberg state
34
35 and the N ground state by the ν_{12} (b_{3u} CH₂ wag) mode, leading to possible internal
36
37 conversion of this Rydberg state towards the ground state. This vibronically induced
38
39 internal conversion could explain the broadening observed in all *ungerade* bands of the
40
41 3s transition, both in absorption [33] and in the present REMPI experiment. A
42
43 substantial vibronic coupling between the $3p_y$ and 3s states, via the ν_8 (b_{2u}) and ν_9 (b_{2u})
44
45 modes, was also predicted in the same work [21]. On the other hand, Rijkenberg and
46
47 Buma [29] concluded to a negligible Rydberg-Rydberg coupling between the *gerade*
48
49 vibronic levels of the 3s and the $3p$ Rydberg states from their PES spectra. This could
50
51 be rationalized again in term of *g-u* “strong propensity rules” for vibronic couplings.
52
53

54
55 As a last remark, ν_3^+ and $\nu_3^+ + 2\nu_4^+$ cation vibrations have been tentatively assigned in
56
57 the spectra of Fig.3 in order to better fit the peak position at 156 meV in panel (a) and
58
59
60

1
2 the broad prominent peak around 200 meV in panel (c). These assignments need to be
3
4 confirmed by better resolved PES spectra, but they seem to indicate some activity in v_3
5
6 upon ionisation from the $3s$ state whereas such activity does not show up upon
7
8 excitation from the neutral ground state to the $3s$ state.
9
10

11 12 13 14 **3.4 The ns - nd Rydberg transition studied via (3+1) photon ionisation**

15
16 [insert Figure 4 about here]
17

18
19 Figure 4 presents the (3+1) REMPI spectrum of ethylene in the 68000-82000 cm^{-1}
20
21 energy region. All assignments are reported in Table 4. It is noticeable that the relative
22
23 intensities in the REMPI spectra of this spectral region are quite different from the ones
24
25 observed in the absorption spectrum (see Fig. 1a), although the peak positions match
26
27 quite well. Some of the bands disappear in the REMPI spectrum or become less intense
28
29 and there is no more obvious regularity in the vibrational structure. The prominence of
30
31 the v_2 and v_2+2v_4 bands observed in the $3s$ transition is no longer observable in the
32
33 higher ns - nd series.
34
35
36

37
38 [insert table 4 about here]
39

40
41 Although our REMPI spectra have been recorded with a much better resolution
42
43 than the absorption spectrum recorded by McDiarmid [14], a similar trend is observed
44
45 in the band broadenings of the one-photon and three-photon spectra. The region of the
46
47 $3d\sigma$ and $3d\delta$ transitions in Fig. 4 exhibits band broadenings similar to the region of the
48
49 $3s$ state studied above (see also Fig. 1). At higher energy, the $4s$ and $4d$ series appear
50
51 with a much broader profile in Fig. 4. Finally for the $5s$ and $5d$ series, the bands present
52
53 a narrower profile though in this high energy region spectral congestion leads to a more
54
55 complicated structure.
56
57
58
59
60

3.4.1. Origin bands

1
2 All origin bands established by McDiarmid from isotopomer analysis [14] are observed
3
4 in the (3+1) REMPI spectra, except for the $4d\delta$ member. At the expected energy of this
5
6 transition, i.e. 77604 cm^{-1} according to Ref. [14], no clear feature shows up in our
7
8 REMPI spectrum. Surprisingly, at slightly higher energy (77795 cm^{-1}), a rather intense
9
10 band could not be assigned in the present work. A careful look at the absorption spectra
11
12 [14] of the different isotopomers indicates the presence of this feature, albeit much
13
14 weaker. This feature has not been assigned so far and cannot be associated with a
15
16 member of a Rydberg series, neither corresponding to an origin band nor to a
17
18 vibrational band.
19
20
21
22

23
24 On the other hand, three new members of the $nd\pi_y$ series have been tentatively
25
26 assigned. The first member, $3d\pi_y$, is located at 66497 cm^{-1} and appears as a very weak
27
28 feature in the REMPI spectrum of Figure 1, indicated by an arrow on panel b). We
29
30 propose here a possible assignment as the $3d\pi_y$ Rydberg state of 1A_u symmetry,
31
32 forbidden by one-photon absorption but allowed by three-photon excitation as indicated
33
34 in Table 5. The corresponding quantum defect of 0.55 (see Table 5), indicative of a
35
36 penetrating orbital, can be rationalized by an occupied precursor orbital in the core for
37
38 this b_{3g} Rydberg orbital, as defined by Mulliken [40]. Further support of our assignment
39
40 is provided by the observation of the $4d\pi_y$ and $5d\pi_y$ features at 75551 and 79165 cm^{-1} ,
41
42 respectively, with identical quantum defect values (see Table 5). Note that a very weak
43
44 feature appeared in the absorption spectrum and was tentatively assigned by McDiarmid
45
46 to a $3p$ forbidden transition, on the basis of the quantum defect value of about 0.5 [14].
47
48
49
50
51
52
53
54

55 3.4.2. Excited vibrational bands

56
57 [insert table 5 about here]
58

59
60 Vibrational bands accompanying the above Rydberg band origins are assigned on the
spectrum of Fig. 4 and reported in Table 4. For comparison, the absorption vibrational

1
2 assignments given by McDiarmid [14] are also reported in this table. These REMPI
3
4 assignments complete the vibrational structure of the Rydberg series, in particular
5
6 through newly assigned ν_3 bands in the $4d\sigma$, $4s$, $5d\sigma$ and $5d\delta$ transitions. A summary of
7
8 the frequencies measured in the present work, namely ν_2 , ν_3 and $2\nu_4$, is presented in
9
10 Table 5, together with the frequency values of Ref. [14], in parenthesis, and with the
11
12 electronic origin energies and quantum defects of the observed ns and nd series. When n
13
14 increases from 3 to 5, the three mode frequencies get closer to the cation $C_2H_4^+$ values
15
16 [32], with the exception of the ν_2 frequency for the $4s$ and $5d\sigma$ members, anomalously
17
18 low as compared to the cation value. The $5s$ state, in particular, behaves as a pure
19
20 Rydberg state, with vibrational frequencies very close to that of the cation. Note that the
21
22 spectral features associated to the $5s$ bands shown in Fig. 4 are the narrowest in the
23
24 whole explored range, probably less affected by Rydberg-valence mixing or by internal
25
26 conversion than the other members of the observed series. A recent calculation of the
27
28 Rydberg series of ethylene lead to the conclusion that Rydberg states other than the $^1B_{1u}$
29
30 symmetry are pure Rydberg states [41]. This conclusion should nonetheless be
31
32 tempered, on the basis of the irregular broadening observed in the $n = 4$ to 5 Rydberg
33
34 series, as well as because of the absence of the $4d\delta$ states in the REMPI spectrum of
35
36 Fig. 4. Similar vibronic couplings as the ones invoked for the $3s$ state could possibly
37
38 occur between Rydberg states or between Rydberg states and the N ground state with
39
40 subsequent internal conversion competing with ionisation and affecting both the REMPI
41
42 bandwidths and band intensities.

3.4.3. Rydberg character of the $3d\sigma$ state: Photoelectron spectra

[insert Figure 5 about here]

Three (3+1) REMPI-PES spectra have been recorded in the $3d\sigma$ region and are presented in Figure 5. They correspond to ionisation from the $3d\sigma$ origin (panel a), from

1
2 the $3d\sigma 4^2$ level (panel b) and from the $3d\sigma 2^1$ level (panel c). These PES spectra have
3
4 been recorded with a resolution comparable to that of the $3s$ PES spectra of Fig. 3.
5
6

7 It is interesting to compare the two PES plots of Fig. 3 and Fig. 5. Like in the $3s$
8
9 levels, the $3d\sigma$ PES spectra reveal a vibrational activity upon ionisation, including the
10
11 ν_2^+ and $2\nu_4^+$ modes, but no clear activity appears in the ν_3^+ mode. This absence of ν_3^+
12
13 activity is expected from the very close frequency value of the $3d\sigma$ state and the cation
14
15 ground state (see Table 1 and Table 5). In the case of the $3d\sigma$ state, the ionisation step
16
17 only requires one-photon absorption from the intermediate level, as can be seen in Fig.
18
19 1, hence the PES spectra must reflect the Franck-Condon factors between the
20
21 $3d\sigma$ Rydberg state and the cation ground state. The similarity in the vibrational
22
23 progression for the PES spectra via the two Rydberg states $3s$ and $3d\sigma$, both of $^1B_{3u}$
24
25 symmetry, both penetrating states (quantum defects of 1.00 and 0.32, respectively),
26
27 seems to confirm the non-Rydberg character of the *ungerade* vibrational levels of the $3s$
28
29 state. Table 5 shows that the $2\nu_4$ frequencies of the $3s$ and $3d\sigma$ states are very close, 507
30
31 cm^{-1} and 515 cm^{-1} , respectively, but larger than the $2\nu_4^+$ cation frequency of 438 cm^{-1}
32
33 (Table 1). The PES's of Fig. 3 and Fig. 5 show indeed a similar activity in $2\nu_4^+$. As for
34
35 the ν_2 frequencies, the $3d\sigma$ state value is in between the $3s$ state value and the cation
36
37 value, as shown in Table 5 and Table 1. Appropriately, the ν_2^+ PES vibrational peaks
38
39 show up with less intensity for the $3d\sigma$ state (Fig. 5) than for the $3s$ state (Fig. 3). These
40
41 PES spectra lead therefore to a more qualified conclusion than that of the recent *ab*
42
43 *initio* calculations of Yamamoto *et al.* [41] who predicted a pure Rydberg character for
44
45 these Rydberg states.
46
47
48
49
50
51
52
53
54
55
56
57

58 4. CONCLUDING REMARKS

59 The analysis of the three-photon REMPI spectra of C_2H_4 has confirmed the earlier
60 vibrational assignment of the absorption spectrum by Merer and Shoonveld [33] and by

1
2
3
4
5
6
7
8
9
10
11
12
13
14
15
16
17
18
19
20
21
22
23
24
25
26
27
28
29
30
31
32
33
34
35
36
37
38
39
40
41
42
43
44
45
46
47
48
49
50
51
52
53
54
55
56
57
58
59
60

McDiarmid [14]. The absence of the $V \leftarrow N$ transition in these REMPI spectra has allowed to search for weaker Rydberg vibrational band structures, and to observe new bands involving the ν_3 mode in the $3s$ system, as well as new electronic components of the $3d$ complexes, i.e. the $3d\pi_y$, $4d\pi_y$ and $5d\pi_y$ components, forbidden by one-photon selection rules.

The vibrational ν_2 and $2\nu_4$ frequencies as well as the PES spectra from the lowest *ungerade* vibrational levels of the $3s$ state indicate a deviation from a pure Rydberg character, in contrast with the results obtained earlier by (2+1) REMPI-PES on the *gerade* vibrational levels of the same $3s$ Rydberg state. The same trend, although less pronounced, is observed for the $3d\sigma$ state.

Finally, most of the *ns* and *nd* Rydberg states observed in the present work present a strongly vibrationally dependent behaviour towards ionisation, as can be noted from the relative REMPI band intensities strongly varying with respect to the corresponding absorption features, even in a narrow energy range for which the laser intensity is almost constant. In addition, large variations in band broadening are observed between 57000 and 82000 cm^{-1} . All these observations support the hypothesis of vibronic couplings, either Rydberg-Rydberg or Rydberg-valence couplings, mediated by non-totally symmetric normal modes. Accurate and complete calculations of these non-adiabatic couplings still remain to be done in order to really explain the very complex VUV spectrum of ethylene.

On the other hand, the experimental task should also be pursued, in order to bring more precise experimental evidences of these vibronic couplings. Further work involving REMPI-PES via all the three-photon accessible *ns* and *nd* states ($n=3-6$) for both C_2H_4 and C_2D_4 isotopomers is needed in order to clarify the degree of Rydberg character, or conversely the strength of non-adiabatic couplings affecting these low lying Rydberg states of ethylene.

ACKNOWLEDGMENTS

First of all, two of the authors (D. G. and A.-L. R.) are most grateful to Dr. Ch. Jungen for having shared with them part of his thorough understanding of molecular Rydberg states.

The authors wish to thank Dr S. Douin and Dr T. Pino for their help in the earlier experimental stage. They acknowledge financial support from the “Programme de Physique et Chimie du Milieu Interstellaire” and from the “Programme National de Planétologie” (CNRS). One of the authors (K. A.) acknowledges financial support from the Atomic Energy Commission of Syria.

REFERENCES

- [1] A.J. Merer, R.S. Mulliken. *Chem. Rev.*, **69**, 639 (1969)
- [2] M.B. Robin, *Higher Excited states of Polyatomic Molecules, Vol II*, p. 4, Academic Press, New York, (1975).
- [3] R. McDiarmid. *On the electronic Spectra of Small Linear Polyenes*, p. 177, John Wiley & Sons. Inc. (1999).
- [4] R.S. Mulliken. *Phys. Rev.*, **43**, 279 (1933)
- [5] P.G. Wilkinson, R.S. Mulliken. *J. Chem. Phys.*, **23**, 1895 (1955)
- [6] R. McDiarmid, E. Charney. *J. Chem. Phys.*, **47**, 1517 (1967)
- [7] A.M. Mebel, Y.-T. Chen, S.-H. Lin. *J. Chem. Phys.*, **105**, 9007 (1996)
- [8] A.M. Mebel, M. Hayashi, K.K. Liang, S.H. Lin. *J. Phys. Chem.*, **103**, 10674 (1999)
- [9] M. Ben-Nun, T.J. Martinez. *J. Phys. Chem.*, **103**, 10517 (1999)
- [10] A. Hazra, H.H. Chang, M. Nooijen. *J. Chem. Phys.*, **121**, 2125 (2004)
- [11] R. Borrelli, A. Peluso. *J. Chem. Phys.*, **125**, 194308 (2006)
- [12] P. Farmanara, V. Stert, W. Radloff. *Chem. Phys. Lett.*, **288**, 518 (1998)
- [13] J.M. Mestdagh, J.P. Visticot, M. Elhanine, B. Soep. *J. Chem. Phys.*, **113**, 237 (2000)
- [14] R. McDiarmid. *J. Phys. Chem.*, **84**, 64 (1980)
- [15] R.J. Buenker, S.D. Peyerimhoff. *Chem. Phys. Lett.*, **36**, 415 (1975)
- [16] R.S. Mulliken. *Chem. Phys. Lett.*, **46**, 197 (1977)
- [17] K.B. Wiberg, C.M. Hadad, J.B. Foresman, W.A. Chupka. *J. Phys. Chem.*, **96**, 10756 (1992)
- [18] C. Petrongolo, R.J. Buenker, S.D. Peyerimhoff. *J. Chem. Phys.*, **76**, 3655 (1982)
- [19] C. Petrongolo, R.J. Buenker, S.D. Peyerimhoff. *J. Chem. Phys.*, **78**, 7284 (1983)
- [20] W. Siebrand, F. Zerbetto, M.Z. Zgierski. *Chem. Phys. Lett.*, **174**, 119 (1990)

- 1
2
3
4
5
6
7
8
9
10
11
12
13
14
15
16
17
18
19
20
21
22
23
24
25
26
27
28
29
30
31
32
33
34
35
36
37
38
39
40
41
42
43
44
45
46
47
48
49
50
51
52
53
54
55
56
57
58
59
60
- [21] A.M. Mebel, M. Hayashi, S.H. Lin. *Chem. Phys.Lett.*, **274**, 281 (1997)
- [22] M. Ben-Nun, T.J. Martinez. *Chem. Phys.*, **259**, 237 (2000)
- [23] K.K. Baeck, T.J. Martinez. *Chem. Phys.Lett.*, **375**, 299 (2003)
- [24] M. Barbatti, J. Paier, H. Lischka. *J.Chem.Phys.*, **121**, 11614 (2004)
- [25] C. Jungen. *J. Chem. Phys.*, **53**, 4168 (1970)
- [26] V. Blanchet, S. Boyé, S. Zamith, A. Campos, B. Girard, J. Liévin, D. Gauyacq. *J. Chem. Phys.*, **119**, 3751 (2003)
- [27] A. Gedanken, N.A. Kuebler, M.B. Robin. *J. Chem. Phys.*, **76**, 46 (1982)
- [28] B.A. Williams, T.A. Cool. *J. Chem. Phys.*, **94**, 6358 (1991)
- [29] R.A. Rijkenberg, W.J. Buma. *J. Phys. Chem. A*, **106**, 3727 (2002)
- [30] S. Guizard, N. Shafizadeh, M. Horani, D. Gauyacq. *J. Chem. Phys.*, **94**, 7046 (1991)
- [31] K. Alnama, J.-H. Fillion, D. Gauyacq. *Journal of Quantitative Spectroscopy and Radiative Transfer*, **105**, 139 (2007)
- [32] S. Willitsch, U. Hollenstein, F. Merkt. *J. Chem. Phys.*, **120**, 1761 (2004)
- [33] A.J. Merer, L. Schoonveld. *Can. J. Phys.*, **47**, 1731 (1969)
- [34] S. Boyé, A. Campos, J.H. Fillion, S. Douin, N. Shafizadeh, D. Gauyacq. *Compte-Rendu de Physique de l'Académie des Sciences, Paris*, **5**, 239 (2004)
- [35] A.J. Merer, L. Schoonveld. *J. Chem. Phys.*, **48**, 522 (1968)
- [36] P.D. Foo, K.K. Innes. *J. Chem. Phys.*, **60**, 4582 (1974)
- [37] M.L. Abrams, E.F. Valeev, C.D. Sherrill, T.D. Crawford. *J. Phys. Chem. A*, **106**, 2671 (2002)
- [38] G. Herzberg. *Molecular Spectra and Molecular Structure; III Electronic spectra and electronic structure of polyatomic molecules*, p. 534, Van Nostrand Reinhold, New York (1966).

- 1
2 [39] D.M.P. Holland, D.A. Shaw, M.A. Hayes, L.G. Shpinkova, E.E. Rennie, L.
3
4 Karlsson, P. Baltzer, B. Wannberg. *Chem. Phys.*, **219**, 91 (1997)
5
6
7 [40] R.S. Mulliken. *J. Chem. Phys.*, **66**, 2448 (1977)
8
9 [41] S. Yamamoto, H. Tatewaki. *Chem. Phys.*, **295**, 47 (2003)
10
11 [42] R.J. Sension, B.S. Hudson. *J. Chem. Phys.*, **90**, 1377 (1989)
12
13 [43] J. Duncan, J.L. McKean, P.D. Mallinson. *J. Mol. Spectrosc.*, **45**, 221 (1973)
14
15 [44] X. Xing, M.-K. Bahng, P. Wang, K.-C. Lau, S.J. Baek, C.Y. Ng. *J. Chem. Phys.*,
16
17 **125**, 133304 (2006)
18
19
20
21
22
23
24
25
26
27
28
29
30
31
32
33
34
35
36
37
38
39
40
41
42
43
44
45
46
47
48
49
50
51
52
53
54
55
56
57
58
59
60

Table 1: Experimental vibrational frequencies of the \tilde{X} ground state, $3s$ Rydberg state and \tilde{X}^+ cation ground state of ethylene (in cm^{-1}). Within the symmetry conventions adopted here, the C=C bond is assigned as the z axis and the x axis is perpendicular to the plane of the ground state molecule (see for instance Ref. [42] for a discussion on the many conventions used to describe ethylene normal modes).

Normal mode	Description	D_{2h}	D_2	\tilde{X} ($N, {}^1A_g$) ^{a)}	$3s$ ($R, {}^1B_{3u}$)	\tilde{X}^+ ($D_0, {}^2B_{3u}$)
ν_1	CH s stretch	a_g	a	3026		
ν_2	C=C stretch	a_g	a	1630	1374 ^{b)} 1376 ^{d)}	1487.7 ^{c)} 1488.3 ^{e)}
ν_3	CH ₂ scissors	a_g	a	1342	1211 ^{d)}	1258.7 ^{c)}
ν_4	torsion	a_u	a	1023		83.7 ^{c)} 84.1 ^{e)}
$2\nu_4$					461 ^{b)} 490 ^{d)}	438.2 ^{c)}
$3\nu_4$						764.6 ^{c)}
$4\nu_4$					1153 ^{d)}	1162.1 ^{c)}
ν_5	CH a stretch	b_{1u}	b_1	3021		2978.7 ^{e)}
ν_6	CH ₂ scissors	b_{1u}	b_1	1444		1411.7 ^{e)}
ν_7	CH ₂ wag	b_{2g}	b_2	940		
ν_8	CH a stretch	b_{2u}	b_2	3105		
ν_9	CH ₂ rock	b_{2u}	b_2	826		
ν_{10}	CH stretch	b_{3g}	b_3	3103		
ν_{11}	CH ₂ rock	b_{3g}	b_3	1220		
ν_{12}	CH ₂ wag	b_{3u}	b_3	949		901.3 ^{c)}

a) taken from Ref. [43]

b) taken from Ref. [14]

c) taken from Ref. [32]

d) this work. The ν_2 value is taken from the 2^1_0 band; ν_3 , $2\nu_4$ and $4\nu_4$ are average values derived from the combination bands observed in Fig.2 (see Table 3)

e) taken from Ref. [44]

Table 2: Calculated equilibrium geometrical parameters for the neutral ground state (N, 1A_g), the $3s$ Rydberg state (R, $^1B_{3u}$) and the cation ground state (D_0 , $^2B_{3u}$) of C_2H_4 . Only the pertinent coordinates in relation with the observed vibrational structure are reported in the Table.

Parameter	\tilde{X}^a	$3s^a$	\tilde{X}^{+b}
$R_{C=C}$ [\AA]	1.338	1.402	1.4004
θ_{HCH} scissor [$^\circ$]	116.6	122.4	118.9
$\tau_{C=C}$ torsion [$^\circ$]	0	20	21

^{a)} Mebel *et al.* Ref. [7]

^{b)} Abrams *et al.* Ref. [37]

Table 3: Assignments for the different transitions observed by (3+2) or (4+1) REMPI spectroscopy of ethylene. The observed peak positions are given with $\pm 20 \text{ cm}^{-1}$ accuracy. Energies marked with an asterisk (*) are located on a peak shoulder. Parenthesis indicate the corresponding three-photon energy for a four-photon process.

Observed energy for a 3hv process (cm^{-1})	Observed energy for a 4hv process (cm^{-1})	Assignment (this work)		Ref. [5]
		3hv	4hv	
57333		$3s 0^0$		57336.0
57840		$3s 4^2$		57832.8
(58382)	77843		$4f_1 0^0$	
58490		$3s 4^4$		58420.0*
(58490)	77987		$4f_{11} 0^0$	
58520		$3s 3^1$		
(58696)	78261		$4f_1 4^2$	
58709		$3s 2^1$		58706.3
(58809)	78412*		$4f_{11} 4^2$	
59200		$3s 2^1 4^2$		59199.1
(59253)	79004*		$4f_1 4^4$	
(59324)	79096		$4f_1 3^1$	
(59450)	79267		$4f_1 2^1$	
(59636)	79515		$4f_1 3^1 4^2$	
59894		$3s 2^1 4^4$		59904.7*
59941		$3s 2^1 3^1$		
60057		$3s 2^2$		60055.4
(60242)	80323		$5f_1 0^0$	
(60345)	80460		$5f_{11} 0^0$	
60535		$3s 2^2 4^2$		60513.2
(60557)	80743		$5f_1 4^2$	
61207		$3s 2^2 4^4$		61226.0*
61270		$3s 2^2 3^1$		
61367		$3s 2^3$		61379.1
61849		$3s 2^3 4^2$		61838.6
62485*		$3s 2^3 4^4$		62547.0*
62580		$3s 2^3 3^1$		
62707		$3s 2^4$		62689.5

Table 4: Assignments for the different *ns-nd* series of ethylene observed by (3+1) REMPI spectroscopy. Transitions located on a shoulder are indicated by an asterisk (*).

Observed three-photon energy (cm ⁻¹)	Ref. [14]	Tentative assignment	Observed three-photon energy (cm ⁻¹)	Ref.[14]	Tentative assignment
68687		unassigned	76500	-	4s 2 ² 4 ²
69530	69531	3dσ 0 ⁰	76753	76728	4dσ 0 ⁰
70045	70033	3dσ 4 ²	77010	-	4dπ _y 2 ¹
70793*	70746	3dσ 3 ¹	77213	77204	4dσ 4 ²
70931	70887	3dσ 2 ¹	-	77604	4dδ 0 ⁰
71437	-	3dσ 2 ¹ 4 ²	77795		unassigned
71782	71813	3dδ 0 ⁰	77945	-	4dσ 3 ¹
71976	-	3dσ 2 ¹ 3 ¹	77945	77912	4dδ 4 ²
72150	72182	3dδ 4 ²	78155	-	4dσ 2 ¹
72355	-	3dσ 2 ²	78302	78302	5s 0 ⁰
72837	-	3dσ 2 ² 4 ²	78558		4dσ 2 ¹ 4 ²
73038	73025	3dδ 3 ¹	78741	78728	5s 4 ²
73260*	73228	3dδ 2 ¹	78985	78970	4dδ 2 ¹
73290*	-	4s 0 ⁰	79165	-	5dπ _y 0 ⁰
73552*		3dσ 2 ² 3 ¹	79553	-	4dσ 2 ²
73730	-	4s 4 ²	79553	79548	5s 3 ¹
73730	-	3dδ 2 ¹ 4 ²	79604		5dπ _y 4 ²
73730	-	3dσ 2 ³	79797	-	5dσ 0 ⁰
74282		3dσ 2 ³ 4 ²	79797	79796	5s 2 ¹

74434	-	$4s\ 3^1$	80227	80222	$5s\ 2^1 4^2$
74434	74440	$3d\delta\ 2^1 3^1$	80227	-	$5d\sigma\ 4^2$
74590	-	$4s\ 2^1$	80227	80218	$5d\delta\ 0^0$
74590	-	$3d\delta\ 2^2$	80423	-	$4d\delta\ 2^2$
74979	-	$3d\sigma\ 2^3 3^1$	80626	80632	$5d\delta\ 4^2$
75256	-	$3d\sigma\ 2^4$	81033	-	$5d\sigma\ 3^1$
75256		$3d\delta\ 2^2 4^2$	81186	-	$5d\sigma\ 2^1$
75551	-	$4d\pi_y\ 0^0$			
75815	-	$4s\ 2^1 3^1$	81186	-	$5s\ 2^2$
76100*	-	$4d\pi_y\ 4^2$	81472	-	$5d\delta\ 3^1$
76100*	-	$4s\ 2^2$	81733	-	$5d\sigma\ 2^1 4^2$
76500	-	$3d\delta\ 2^3 4^2$			

Table 5: Quantum defects (δ) and observed vibrational level differences (in cm^{-1}) of ns and nd Rydberg states of C_2H_4 . δ is calculated by using the well-known Rydberg formula: $\delta = n - [\text{Ry}/(\text{IP}-E)]^{1/2}$ where n is the principal quantum number, $\text{Ry} = 109735 \text{ cm}^{-1}$, $\text{IP} = 84790.4 \text{ cm}^{-1}$ (Ref. [32]) and E is the origin band energy of the Rydberg state in cm^{-1} . Frequencies are reported within $\pm 30 \text{ cm}^{-1}$. Values in parenthesis are taken from Ref. [14]. The asterisk indicates transitions forbidden by one-photon absorption.

State	D_{2h} Symmetry	Energy 0_0^0	δ	2_0^1	3_0^1	4_0^2
$3s$	B_{3u}	57333	1.00	1376	1187	507
				(1374)		(461)
$4s$	B_{3u}	73290	0.91	1300	1144	440
$5s$	B_{3u}	78302	0.89	1495	1251	439
				(1494)	(1246)	(426)
$3d\sigma$	B_{3u}	69530	0.32	1401	1263	515
				(1356)	(1215)	(502)
$4d\sigma$	B_{3u}	76753	0.30	1402	1192	460
						(476)
$5d\sigma$	B_{3u}	79797	0.31	1389	1236	430
$3d\pi_y$	A_u^*	66497	0.55	-	-	-
$4d\pi_y$	A_u^*	75551	0.55	1459	-	549
$5d\pi_y$	A_u^*	79165	0.58	-	-	439
$3d\delta$	B_{2u}	71782	0.096	1478	1256	368
				(1415)	(1212)	(369)
$4d\delta$	B_{2u}	(77604)	-	1381	-	341
				(1366)	(1242)	(308)
$5d\delta$	B_{2u}	80227	0.096	-	1245	399
						(414)

FIGURE CAPTIONS

Figure 1: Survey of: (panel a) the one-photon absorption spectrum recorded in this work, (panel b) the three-photon REMPI spectrum of ethylene in the 56000-88000 cm^{-1} three-photon energy region, without any laser intensity corrections, and (panel c) the corresponding dye laser curves. Note that in the region below 63593 cm^{-1} , absorption of two photons is required for ionisation. Note also that in the (3+2) REMPI region, the $V \leftarrow N$ transition disappears from the REMPI signal, leaving only the vibrational structure of the $3s \leftarrow N$ system. The arrow displayed at 66497 cm^{-1} on panel (b) indicates the position of the $3d\pi_y$ origin band.

Figure 2: Region of the $3s$ Rydberg state probed by (3+2) REMPI spectroscopy in the range 56500-63000 cm^{-1} together with the vibrational assignments involving progressions in ν_2 , $\nu_2+2\nu_4$, $\nu_2+4\nu_4$ and $\nu_2+\nu_3$. The three-photon effective resolution of these scans is about 1 cm^{-1} . Note that the two scans used to cover the related spectral range of the spectrum (56500-61700 cm^{-1} and 59500-63000 cm^{-1}) have not been corrected from the laser intensity but have been approximately normalised to each other by overlapping of the $3s$ 2^24^2 bands. Tentative assignments for nf Rydberg series observed by (4+1) REMPI spectroscopy are also reported on the spectrum with the corresponding four-photon energy scale at the top of the plot.

Figure 3: (3+2) REMPI-PES spectra of the $3s$ Rydberg state for: (a) the origin band at 57333 cm^{-1} , (b) the $2\nu_4$ vibrational band at 57840 cm^{-1} , and (c) the ν_2 vibrational band at 58709 cm^{-1} . The poor energy resolution (about 90 meV) is probably due to space charge effects occurring in the interaction volume, but a vibrational structure of the cation is still detectable in the three spectra. Note that at negative ion energy, two vibrational

1
2 peaks appear in the spectrum of panel (a) and can be associated with six-photon
3
4 ionisation [most probably (3+3)] into the \tilde{A} state of the $C_2H_4^+$ cation (origin band+first
5
6 vibrational level as given in Ref. [39]). The occurrence of prominent overlapping
7
8 vibrational PES peaks in the cation explains the increasing broadening of the principal
9
10 vibrational PES peaks in the cation explains the increasing broadening of the principal
11
12 peak around zero ion internal energy from panel (a) to (c).
13
14

15
16 **Figure 4:** Region of the *ns-nd* Rydberg series probed by (3+1) REMPI spectroscopy in
17
18 the range 68000-82000 cm^{-1} . The vibrational assignments reported on the graph as a
19
20 triplet (*m n p*) corresponds to the combination bands $mv_2+nv_3+pv_4$. In addition,
21
22 tentative assignments for the $4d\pi_y$ and $5d\pi_y$ states are reported on the spectrum. Various
23
24 band broadenings are observed in these spectra, all recorded with the same three-photon
25
26 band broadenings are observed in these spectra, all recorded with the same three-photon
27
28 effective resolution of 1 cm^{-1} . The question mark indicates the expected position of the
29
30 unobserved $4d\delta$ band (at 77604 cm^{-1} according to Ref. [14]).
31
32
33
34
35

36 **Figure 5:** (3+1) REMPI-PES spectra of the $3d\sigma$ Rydberg state for: (a) the origin band at
37
38 69530 cm^{-1} , (b) the $2v_4$ vibrational band at 70045 cm^{-1} , and (c) the v_2 vibrational band at
39
40 70931 cm^{-1} . These three spectra exhibit a significant activity in the $2v_4^+$ mode as
41
42 compared to the v_2^+ and v_3^+ modes more prominent in the $3s$ PES spectra of Figs 3. The
43
44 energy resolution is similar to that of Fig. 3, i.e. 90 meV at best, in the zero ion energy
45
46 region.
47
48
49
50
51
52
53
54
55
56
57
58
59
60

Figure 1

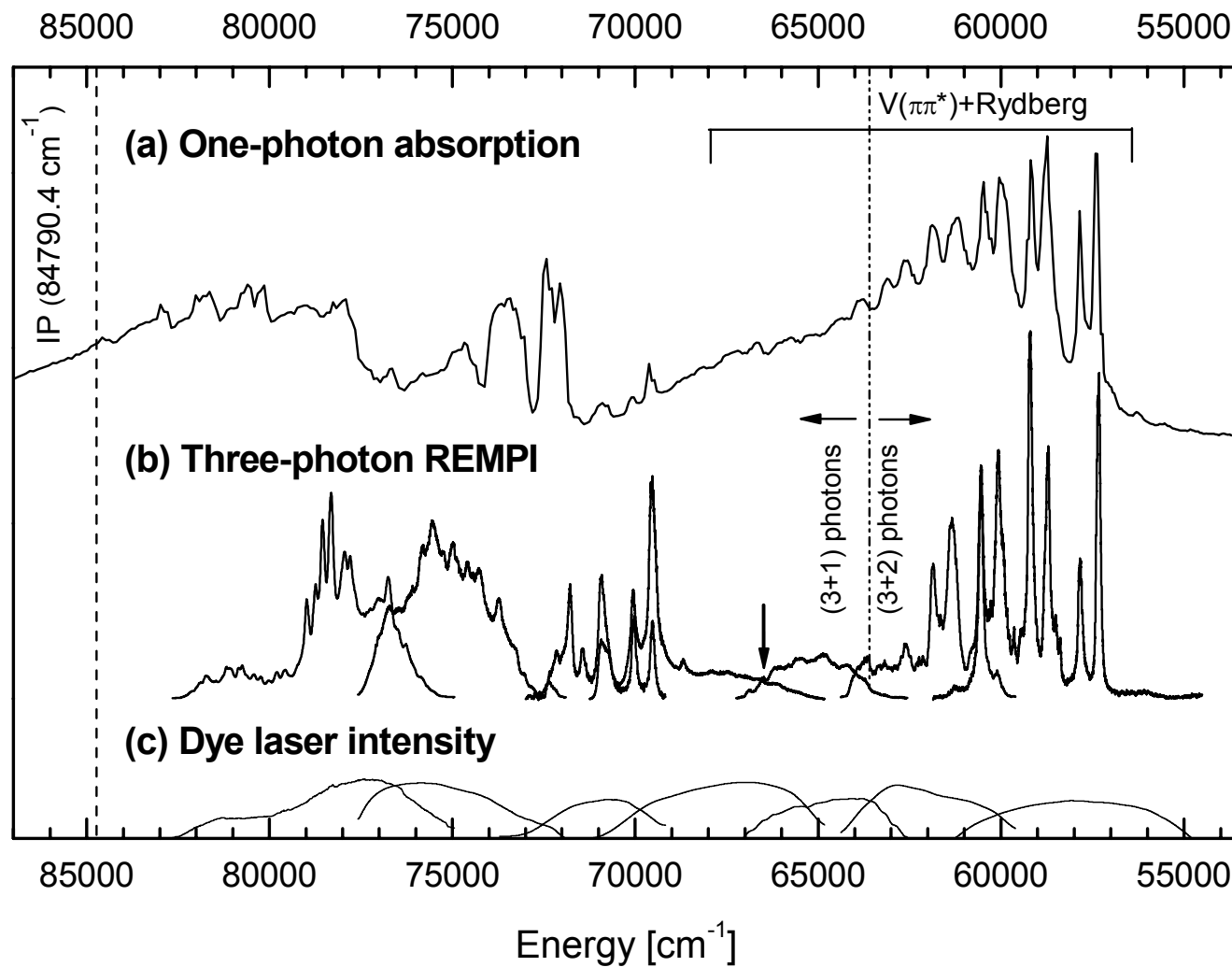


Figure 2

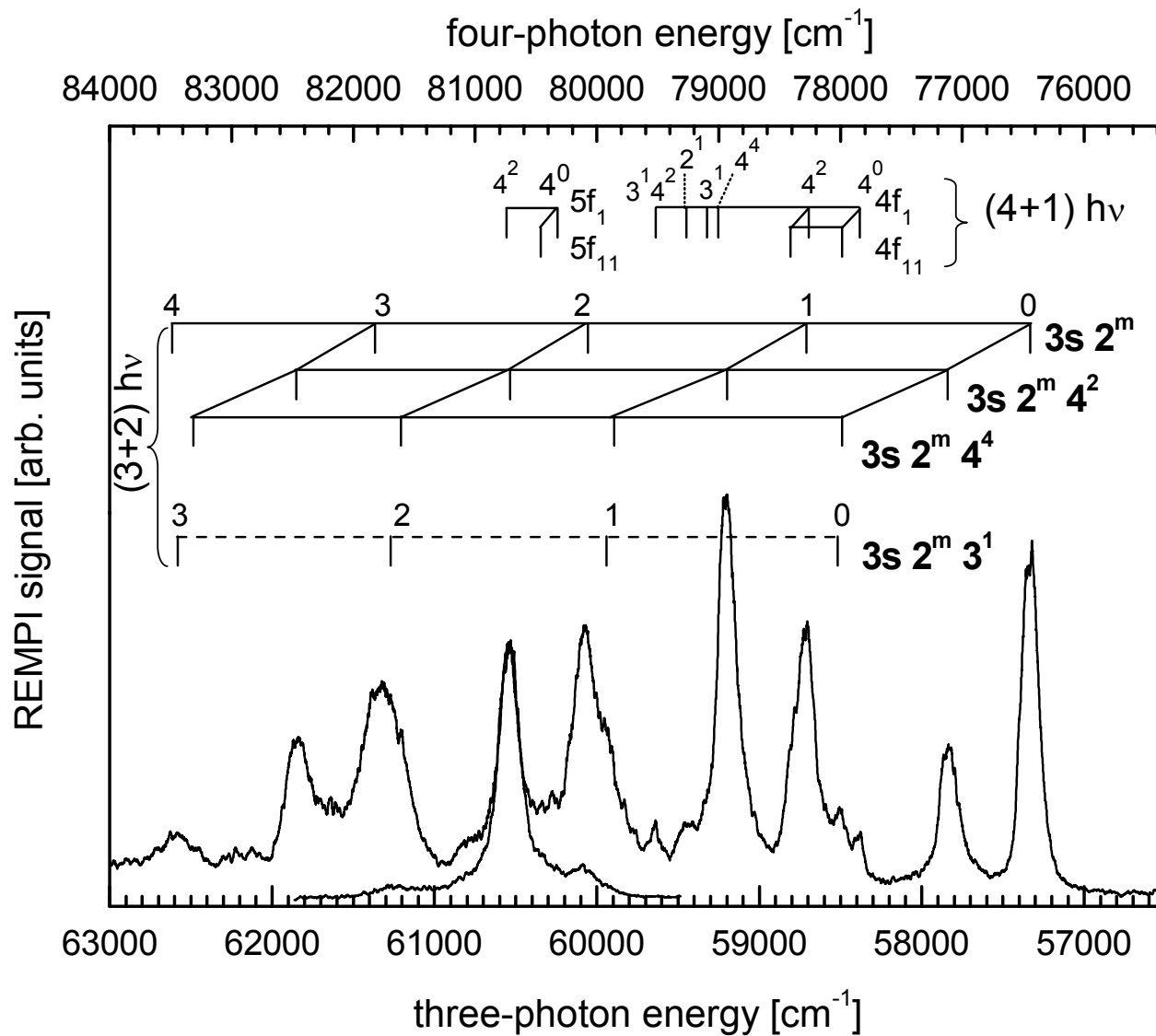


Figure 3

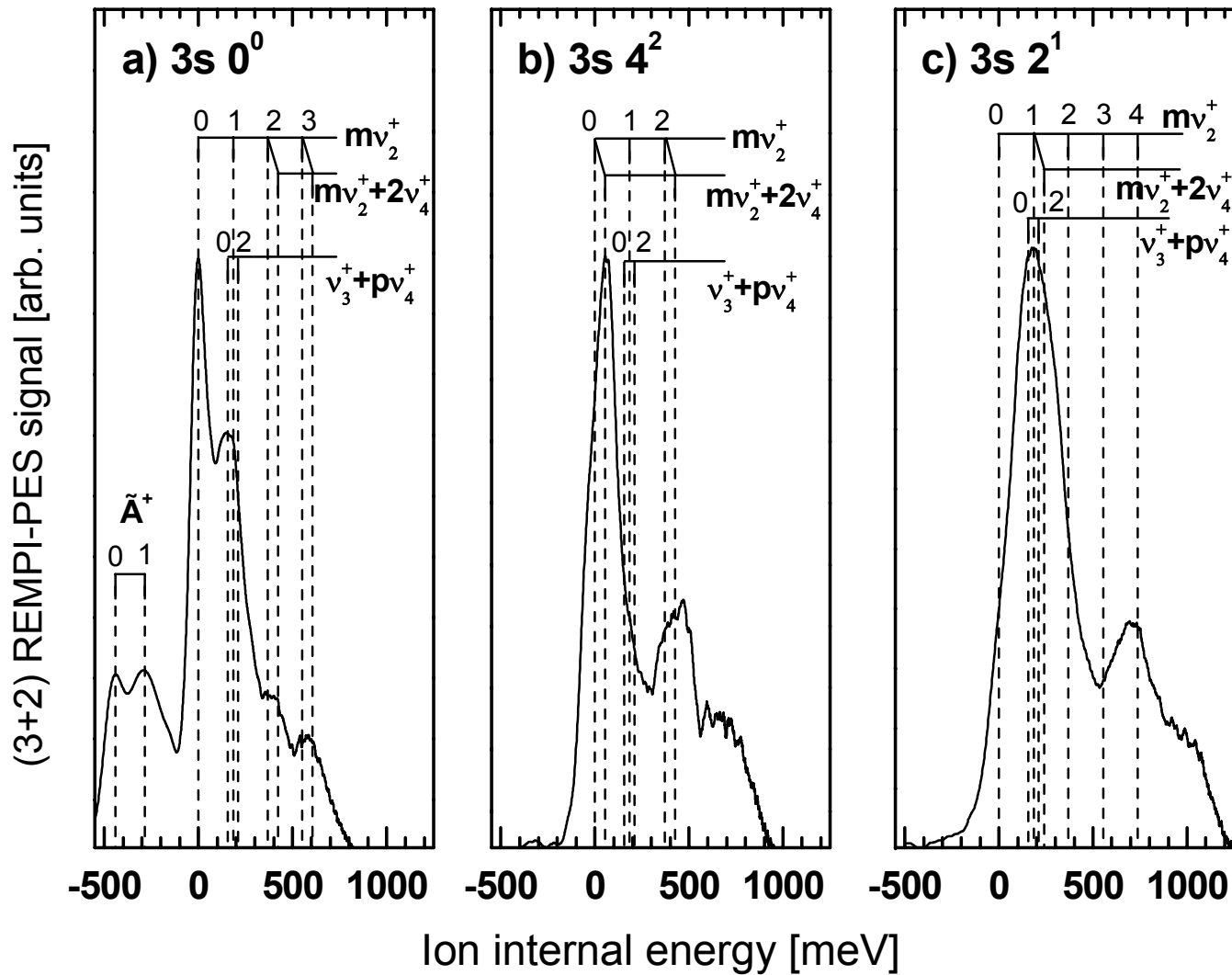


Figure 4

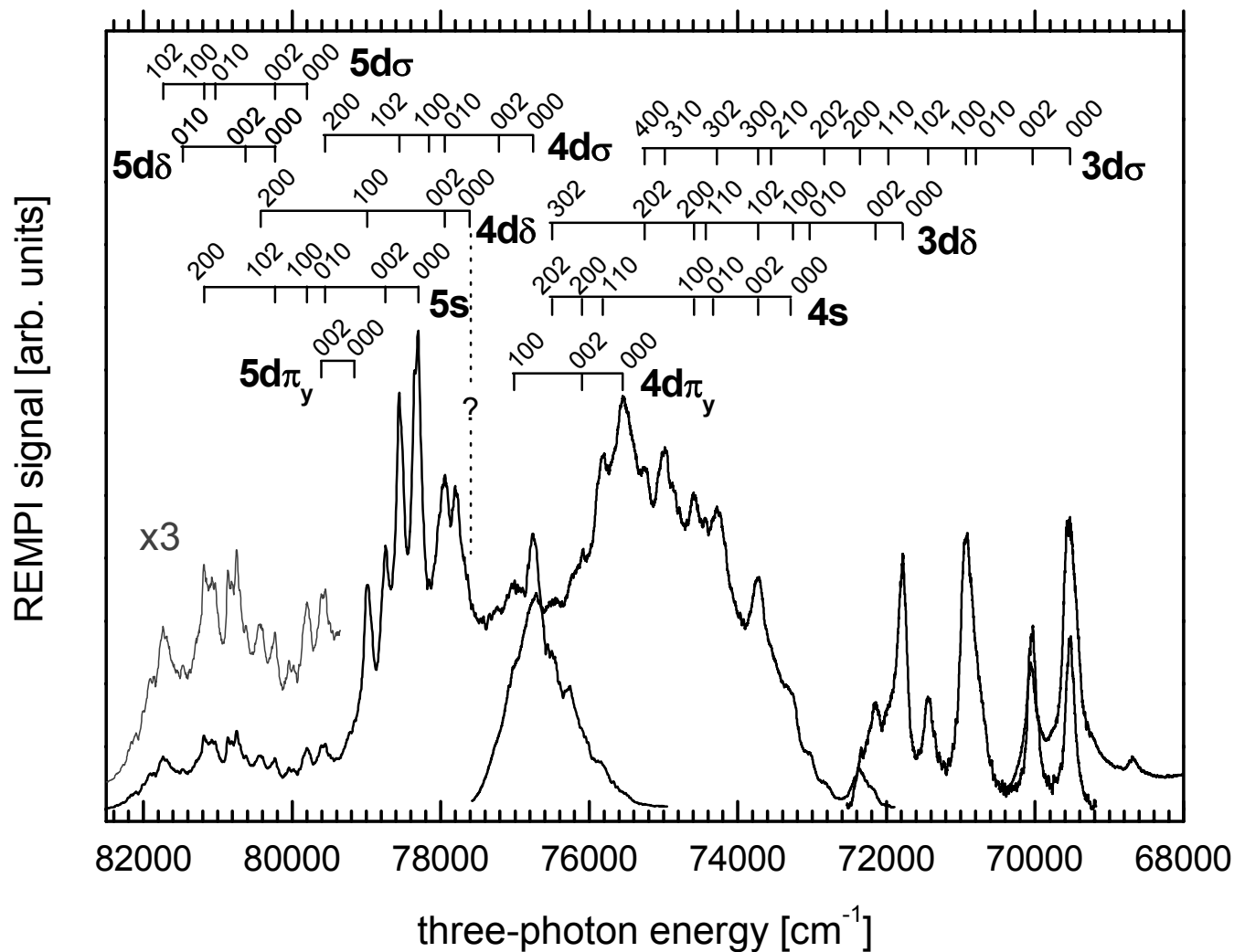
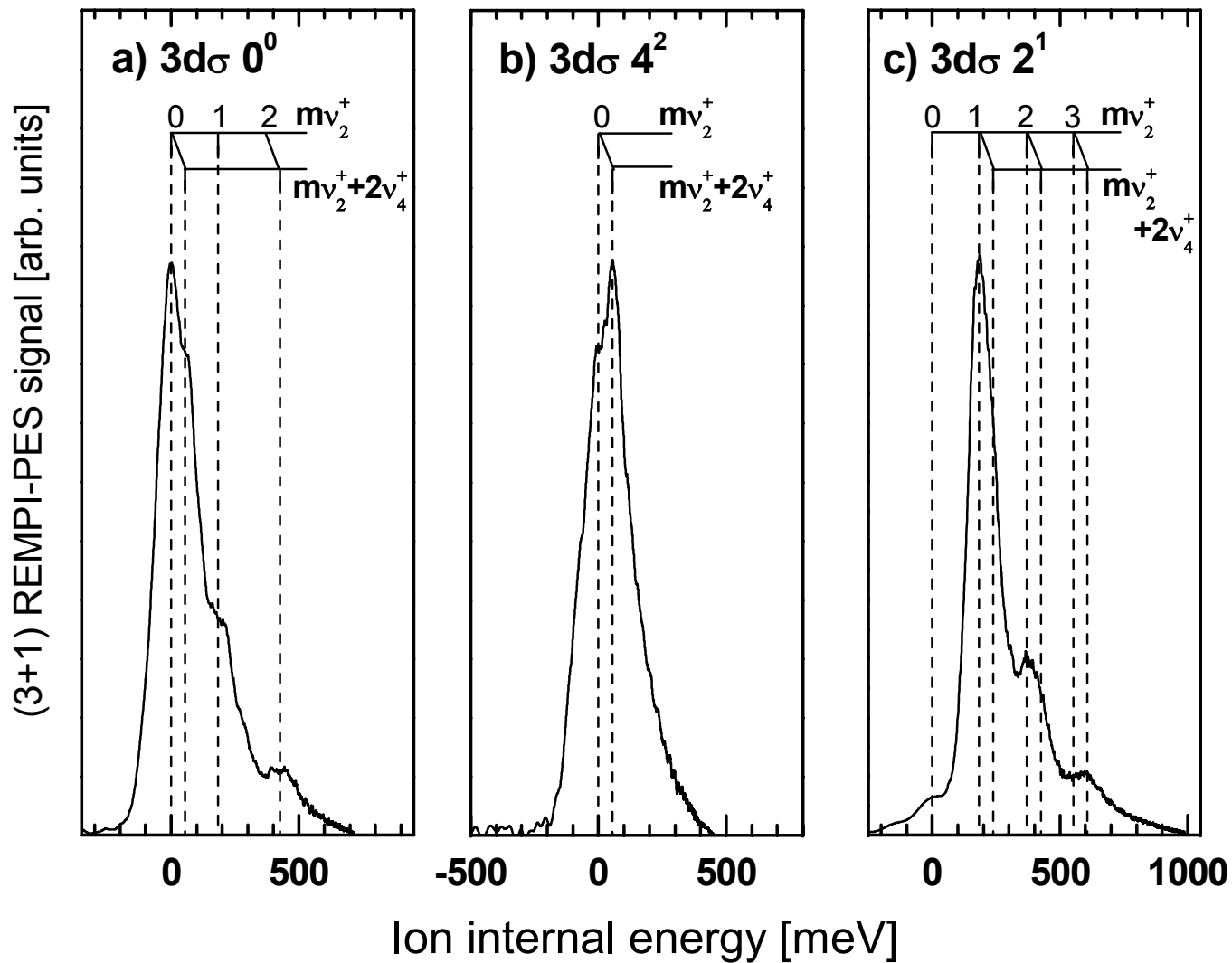


Figure 5



1
2
3
4
5 **Excited states of C₂H₄ studied by (3+1) and (3+2) REMPI**
6
7 **spectroscopy: disentangling the lowest Rydberg series**
8
9
10 **from the strong $\pi\text{-}\pi^*$ V \leftarrow N transition**
11
12

13
14
15
16 **(Shortened version of the title: Three-photon REMPI spectra of C₂H₄)**
17
18
19
20

21
22 K. ALNAMA^{a),b)}, S. BOYÉ-PÉRONNE^{a)}, A.-L. ROCHE^{a)}, and D. GAUYACQ^{*a)}
23
24

25
26
27 a) Laboratoire de Photophysique Moléculaire, CNRS UPR 3361, Bât. 210,
28

29
30 Université Paris-Sud, 91405 Orsay Cédex, France

31
32 b) Permanent address: Atomic Energy Commission of Syria, P.O. BOX 6091, Damascus, Syria
33
34

35
36
37 *Corresponding author. Telephone: (+33) 1 69156307; Fax: (+33) 1 69156777; E-mail:
38

39 dolores.gauyacq@ppm.u-psud.fr
40
41
42
43
44
45
46
47
48
49
50
51
52
53
54
55
56
57
58
59
60

(3+1) and (3+2) Resonantly Enhanced Multiphoton (REMPI) spectroscopy has been carried out to study the Rydberg states of C₂H₄ in the region 55000-83000 cm⁻¹. Differences and similarities were observed between these three-photon spectra and the one-photon absorption spectrum. First, the disappearance of the strong $\pi\text{-}\pi^*$ V \leftarrow N valence transition from the REMPI spectra allowed to disentangle the vibrational structure of the 3s Rydberg transition from the V \leftarrow N quasi-continuum, and to search for additional weak transitions. Earlier vibrational assignments from the absorption spectrum have been confirmed in the REMPI analysis of the 3s \leftarrow N and ns,nd \leftarrow N transition systems, although with very different band intensities. This analysis has provided additional weak band assignments involving the ν_3 mode in the observed Rydberg transitions. New electronic components (3d π_y , 4d π_y , 5d π_y) of the nd complex which are three-photon allowed but one-photon forbidden, have been tentatively assigned. The photoelectron (PES) spectra of the 3s and 3d σ lowest vibrational levels have revealed a deviation from a pure Rydberg character, in apparent contradiction with previous (2+1) REMPI-PES data involving *gerade* vibronic levels of the 3s Rydberg state, which led to a prominent Rydberg character for this state. Rydberg-valence and Rydberg-Rydberg vibronic interactions mediated via non-symmetric modes could explain the different behaviour between *gerade* and *ungerade* vibronic levels of the ethylene Rydberg states.

Keywords: ethylene; Rydberg states; REMPI spectroscopy; REMPI-PES

1. INTRODUCTION

Although the ethylene molecule is of fundamental interest both for organic photochemistry and for electronic structure theory, our understanding of the spectroscopy of this molecule is far from complete [1],[2,3]. Despite decades of spectroscopic investigations and electronic structure calculations, many questions remain unanswered concerning the assignment of the vacuum-ultraviolet (VUV) spectrum of ethylene. Indeed the absorption spectrum exhibits severe overlapping of valence-valence and Rydberg-valence transitions with the appearance of many diffuse vibrational bands. According to Mulliken's notations [4], the ground state and lowest valence excited states are designed as N (for normal), V (for the $\pi\pi^*$ Valence) and Z (for the π^{*2} Zwitterionic), while the lowest Rydberg state, the $3s$ state, is designed as R. The $\pi-\pi^*$, $V \ ^1B_{1u} \leftarrow N \ ^1A_g$ transition exhibits an extremely extended quasi-continuum, with a broad vibrational structure which has been the subject of many questions, including the effect of Duschinsky rotation and the effect of the large amplitude torsional mode [5],[6],[7],[8],[9],[10],[11]. Recently, new dynamic information has been obtained by femtosecond pump-probe spectroscopy in the region around 6 eV [12],[13]. The lifetime of the $\pi\pi^*$ V state has been determined as 30 ± 15 fs [12] and 20 ± 10 fs [13], in agreement with the broad vibrational bands, showing a typical bandwidth of about 400 cm^{-1} .

Concerning the absorption transitions towards Rydberg states, the electronic origin bands of the ns and nd states and their vibrational progressions have been observed with sharper profiles than those of the $V\leftarrow N$ transition, although they all present some spectral broadening. The analysis of the ethylene Rydberg transitions, as compared for instance to linear acetylene, has been proved non trivial due to the large geometry change between the ground state, the Rydberg states and the cationic ground state. The most complete vibrational analysis of the ns and nd Rydberg transitions

1 including partially or totally deuterated isotopomers has been performed by McDiarmid
2 [14]. This analysis allowed unambiguous assignments of several ns and nd band origins
3
4
5
6 from $n=3$ to 6. Nevertheless, some absorption features remained unexplained or
7
8 tentatively assigned. Table 1 recalls the definition of the twelve normal modes of
9
10 ethylene with the symmetry conventions adopted in the present paper. The most active
11
12 bands in the Rydberg absorption transitions involve the ν_4 torsion mode and the ν_2 CC
13
14 stretching mode. In addition, bands involving the ν_3 CH₂ scissors mode have also been
15
16 observed, though with a weaker intensity.
17
18
19

20
21 [insert table 1 about here]
22

23
24 Rydberg-valence interactions in ethylene have been the subject of many
25
26 theoretical investigations [15],[16],[17],[18],[19],[20],[21],[22],[23],[24]. Indeed, the
27
28 observation of Rydberg transitions in the same region as the $V \ ^1B_{1u} \leftarrow N \ ^1A_g$ transition
29
30 opened a question about a valence-Rydberg interaction through vibronic coupling,
31
32 already addressed in the earlier work of Wilkinson and Mulliken [5]. Buenker and
33
34 Peyerimhoff [15] found a Rydberg-valence mixing between the $V \ ^1B_{1u}$ state and the
35
36 $3d\pi_x \ ^1B_{1u}$ state calculated by *ab initio* approaches, which was the beginning of a
37
38 longstanding controversy on the Rydberg character of the V state: Mulliken discussed in
39
40 detail this point, by considering the concept of core molecular orbital precursors for
41
42 describing the Rydberg molecular orbitals, and rejected the existence of two separate V
43
44 and $3d\pi_x$ states [16]. In the case of NO, Jungen [25] has discussed a similar situation
45
46 through a very insightful paper which clearly highlights Mulliken's concept of precursor
47
48 in Rydberg orbitals. The ethylene controversy was summarized later on by Wiberg *et al.*
49
50 [17] who, again by considering Mulliken's precursor definition, reconciled the point of
51
52 view of Buenker and Peyerimhoff [15] and that of Mulliken [16]. Petrongolo *et al.*
53
54 [18],[19] calculated another important nonadiabatic coupling between the $V \ ^1B_{1u}$ state
55
56 and the $3p_y \ ^1B_{1g}$ Rydberg state, via the torsional coordinate of a_u symmetry. Later on,
57
58
59
60

1 Siebrand *et al.* [20] proposed a vibronic coupling between the V $^1B_{1u}$ state and the
2 lowest $3s$ $^1B_{3u}$ Rydberg state via the ν_7 wagging mode (b_{2g} symmetry as defined in
3 Table 1). More recently, this vibronic coupling has been reinvestigated by Mebel *et al.*
4 [21], who found, in addition, a significant intra-Rydberg vibronic coupling between the
5 $3p_y$ and the $3s$ states via the ν_8 and ν_9 modes (with the definition of Table 1).
6 Interestingly, these authors also studied the internal conversion both from the $\pi\pi^*$ V
7 state and from the $3s$ state towards the ground state.
8

9
10
11
12
13
14
15
16
17
18
19 Very accurate *ab initio* calculations have been performed on the low lying
20 Rydberg states embedded in the valence V state of C_2H_4 , in particular in the vertical
21 excitation region from the planar ground state zero energy up to 8 eV
22 [7],[9],[21],[22],[23],[24]. In some of these latter studies [21],[22],[23],[24], several
23 conical intersections connecting the V state to low lying Rydberg states have been
24 identified, yet without providing further details on Rydberg-valence interactions.
25
26
27
28
29
30
31
32

33
34
35
36
37
38
39
40
41
42
43
44
45
46
47
48
49
50
51
52
53
54
55
56
57
58
59
60
The present work focuses on the Rydberg state analysis via three-photon
excitation, multiphoton ionisation. Resonantly-enhanced multiphoton ionisation
(REMPI) and photoelectron spectroscopy (REMPI-PES) spectra have been proved very
efficient for extracting information on the Rydberg character and the Rydberg-valence
interaction (see for instance Ref. [26] in the case of acetylene). Surprisingly, very few
REMPI studies have been performed on ethylene, except for two-photon excitation
studies, which have revealed the structure of the gerade np and nf states [27],[28],[29].
In one of these two-photon studies, vibronic bands involving odd quanta of ν_4 for the $3s$
Rydberg state have also been observed [29].

To our knowledge, no three-photon REMPI spectra of ethylene have been
reported yet in the literature. These three-photon spectra bring pieces of information
complementary to the absorption spectrum:

- 1
2
3
4
5
6
7
8
9
10
11
12
13
14
15
16
17
18
19
20
21
22
23
24
25
26
27
- i) The REMPI technique strongly favours observation of the Rydberg states with respect to excited valence states: indeed, the Rydberg electron is easily ionised by the last photon, and moreover, very unstable valence states decay much faster than they ionise, and cannot be observed by ionisation with the typical laser power density used in REMPI spectroscopy.
 - ii) The three-photon spectra almost share the same selection rules with the one-photon absorption spectrum (odd number of photons). Hence observation of the ns and nd Rydberg states is strongly allowed and can shed light on some questionable assignments of the absorption spectrum. Moreover, additional symmetry-allowed transitions can be observed, such as A_u vibronic levels.

28
29
30
31
32
33
34
35
36
37
38
39
40
41

This paper presents a detailed vibrational analysis of the observed (3+1) and (3+2) REMPI spectra of C_2H_4 in the 55000-83000 cm^{-1} three-photon energy region. REMPI-PES spectra have also been recorded from resonant $3s$ and $3d$ vibronic levels and are discussed with respect to the Rydberg character of these low-lying Rydberg states, as well as in the context of possible Rydberg-valence interactions.

42 2. EXPERIMENTAL

43
44
45
46
47
48
49
50
51
52
53
54
55
56
57
58
59
60

The (3+1) and (3+2) REMPI experiments were performed in a magnetic bottle electron spectrometer, described elsewhere [30]. Ethylene was introduced into a vacuum chamber through a 2-mm diameter hole. The typical background pressure was 8.10^{-5} mbar in the interaction region, so that an effusive beam condition allowed for moderate rotational cooling of the molecules (170K-typical rotational temperature). Tuneable radiation was generated by an excimer (XeCl, LUMONICS PM 886) pumped dye laser (Lambda Physik FL2002) operating with different dye solutions covering the spectral region 538-360 nm (coumarin 500, coumarin 480, coumarin 460, coumarin 440, furan

1
2
3
4
5
6
7
8
9
10
11
12
13
14
15
16
17
18
19
20
21
22
23
24
25
26
27
28
29
30
31
32
33
34
35
36
37
38
39
40
41
42
43
44
45
46
47
48
49
50
51
52
53
54
55
56
57
58
59
60

1, PBBO and QUI), with a typical bandwidth of 0.3 cm^{-1} for one-photon energy. The laser beam was focused with a 150 mm focal length lens. The laser energy at the entrance of the magnetic bottle varied between 3 mJ and 7 mJ per pulse for the spectral region corresponding to a (3+1) photon ionisation process, depending on the dye solution. For the (3+2) photon ionisation process, energies between 5 and 10 mJ per pulse were used. The laser was operating at 10 Hz with a typical pulse duration of 10 ns. Two different spectra were recorded:

(i) The total photoelectron signal was collected as a function of the laser wavelength by a microchannel plate detection system. An appropriate time-gate selected the electrons produced by the (3+1) or (3+2) ionisation process in ethylene, and the signal was accumulated over about 10 laser shots. The photon wavelength was calibrated in the $55000\text{-}83000 \text{ cm}^{-1}$ three-photon energy region by recording the optogalvanic spectrum of an iron-neon hollow cathode [31]. It should be noted that many spectral features present quite broad linewidths. Although the absolute accuracy of the quoted energies is $\pm 1 \text{ cm}^{-1}$, the broadening of the observed bands and the strong overlap in these regions lead to an estimated precision on the vibrational band positions of $\pm 20 \text{ cm}^{-1}$.

(ii) Time-of-flight photoelectron spectra were recorded at fixed three-photon wavelengths. Careful energy calibration of these PES spectra was performed by constructing a calibration curve from the (3+1) REMPI-PES signal via the $3d\sigma$ origin band of ethylene recorded at different retarding bias voltages V_g . The calibration was performed following the law:

$$E_{kin} = \left(\frac{A}{t_{TOF} - t_0} \right)^2 - V_0 - V_g \quad (1)$$

where E_{kin} is the kinetic energy of the photoelectrons in eV, t_{TOF} is their arrival time at the detector in nanoseconds, t_0 (in ns) and V_0 (in V) are time and voltage parameters,

1
2 and A is a geometrical parameter of the magnetic bottle ($A = 844 \text{ eV}^{1/2} \cdot \text{ns}$). The best
3
4 PES spectra have been obtained by accumulating the signal over 3000 laser shots, and
5
6 by applying a moderate retarding bias voltage, between -0.06 V and -0.4 V , insuring a
7
8 compromise between electron energy resolution (around 90 meV at low kinetic energy)
9
10 and photoelectron signal detection threshold.
11
12

13
14
15 For comparison with the present REMPI spectra, the one-photon VUV
16
17 absorption spectrum of C_2H_4 has been recorded over the same excitation range at the
18
19 synchrotron radiation facility in Orsay (Super-ACO) on the SA63 beam line. The SA63
20
21 beam line was equipped with a 3-m Eagle normal incidence monochromator and a 1800
22
23 grooves/mm grating tuned in the 188-112 nm spectral region with a 0.08 nm resolution
24
25 (i.e. $60\text{-}70 \text{ cm}^{-1}$). In the experiment performed with this beamline, ethylene was
26
27 introduced into a vacuum chamber by means of a stainless steel needle with a $100\text{-}\mu\text{m}$
28
29 internal diameter, and excited by the VUV beam. A background pressure of about 10^{-4}
30
31 mbar was maintained in the vacuum chamber. The transmitted VUV light was recorded
32
33 through the visible fluorescence of a coated sodium salicylate window and collected by
34
35 a photomultiplier tube (Hamamatsu R928, spectral range 950-185 nm).
36
37
38
39
40
41
42
43
44

45 3. RESULTS AND DISCUSSION

46 3.1. Brief summary on the selection rules in REMPI spectra

47
48 As was pointed out by Willitsch *et al.* [32], in the case of the twisted cation ground state
49
50 of ethylene, the adequate molecular symmetry group remains D_{2h} . The same symmetry
51
52 prescription holds for all Rydberg states of neutral ethylene converging to the cation
53
54 ground state, for which the robust g/u symmetry has been noticed to govern the whole
55
56 absorption spectrum [14]. Therefore, the REMPI spectroscopy can be divided in two
57
58
59
60

1
2 groups of experiments depending on the number of photons involved in the excitation
3
4 step.

5
6
7 (i) *one-photon and three-photon excitation*: From the neutral ground state 1A_g , only
8
9 vibronic levels of $^1B_{1u}$, $^1B_{2u}$ and $^1B_{3u}$ are accessible in one-photon. In addition,
10
11 vibronic levels 1A_u symmetry are also accessible by three-photon excitation. This is
12
13 why the present (3+2) and (3+1) spectra are dominated by the same vibronic
14
15 structure as the absorption spectrum, as will be shown in the following sections.

16
17
18 (ii) *two-photon and four-photon excitation*: From the neutral ground state 1A_g , only
19
20 vibronic levels of 1A_g , $^1B_{1g}$, $^1B_{2g}$ and $^1B_{3g}$, are accessible in two- and four-photon
21
22 experiments. This is the case of the (2+1) photon REMPI work of Ref. [29] and of
23
24 the (4+1) photon weak bands observed in the present work and discussed in section
25
26 3.3.2 below.
27
28
29
30
31
32

33 **3.2. Overview of the three-photon excitation spectrum of ethylene**

34
35 Figure 1 presents an overview of the three-photon spectra of ethylene, together with its
36
37 corresponding one-photon absorption spectrum, in the 55000-83000 cm^{-1} three-photon
38
39 energy region. The three-photon spectra have been obtained with seven different dye
40
41 laser solutions and could not be normalised to each other because of poor overlapping
42
43 transitions in the different overlapping dye spectral regions. Inside each spectral region,
44
45 a drastic dependence upon laser intensity is expected and can affect the three-photon
46
47 REMPI intensity spectra, but this dependence has not been studied systematically.
48
49 Consequently, the spectra of Fig.1b have not been corrected from laser intensity and the
50
51 dye laser intensity curves have been added in Fig.1c. Note that in the low energy region
52
53 (i.e. below 63593 cm^{-1}), the ionisation step requires two photons, as shown in Fig. 1.
54
55
56
57
58

59 [insert Figure 1 about here]
60

1
2 If one considers first the one-photon absorption spectrum, the explored spectral
3 range can be divided into two main regions: The low energy range (55000-68000 cm^{-1})
4 exhibits the very strong $V \leftarrow N$ bands superimposed by the sharper vibrational structure
5 of the lowest $3s$ transition. Above 68000 cm^{-1} , the ns and nd Rydberg series show up
6 with more or less diffuse vibrational structures from the $3d\sigma$ origin at 69530 cm^{-1} .
7 Following the pioneering work of Wilkinson and Mulliken [5], this absorption spectrum
8 has been analysed in details by Merer and Schoonveld [33] in the $3s$ transition region,
9 and by McDiarmid [14] for the ns and nd series.
10
11
12
13
14
15
16
17
18
19
20

21 Let us now consider the three-photon REMPI spectra. A very different aspect is
22 observed between the three-photon and the absorption spectra, both in structure and
23 relative intensity, unlike the case of acetylene [34]. In particular, two striking features
24 appear in Fig. 1 by comparison with the one-photon absorption spectrum:
25
26
27
28
29

30 (i) In the 55000-64000 cm^{-1} three-photon energy region, the $V \leftarrow N$ transition is
31 completely absent from the REMPI spectrum. This allows to completely disentangle the
32 vibronic structure of the $3s$ Rydberg state from the underlying $V \leftarrow N$ strong quasi-
33 continuum, and to search for new weaker transitions. Section 3.3 below is devoted to
34 the analysis of these $3s$ vibrational bands.
35
36
37
38
39
40
41

42 (ii) In the 68000-83000 cm^{-1} three-photon energy region, both Rydberg structures
43 and vibrational bands of ns and nd Rydberg states notably differ from the absorption
44 spectrum, making the assignment of the REMPI spectra very difficult at first sight.
45 Some strong features in the absorption spectrum, as the $4d\delta$ origin band at 77604 cm^{-1} ,
46 almost disappear in the REMPI spectra. This is most probably indicative of large
47 variations in the decay dynamics of the Rydberg components in this region, as discussed
48 in section 3.4.
49
50
51
52
53
54
55
56
57
58
59
60

3.3. The 3s Rydberg transition studied via (3+2) photon ionisation

The 3s absorption spectrum has been analysed in detail by Merer and collaborators [35],[33] who established from their analysis the twisted equilibrium geometry of the 3s Rydberg state. These authors derived a value for the torsion angle of 25°, and a value for the inversion barrier to planarity of about 290 cm⁻¹. This twisted geometry is very similar to the one established more recently for the ground state of the C₂H₄⁺ cation, i.e. 29° torsion angle (see Ref. [32] and Table VI therein). Later on, the geometry of the 3s state was reconsidered by Foo and Innes [36], who proposed a different evaluation of the torsion angle of 37°, from the spectral analysis of the 3s absorption spectrum in different isotopomers of ethylene. However, this latter value seems overestimated by comparison with the recently measured cation value [32], and also by comparison with recent *ab initio* calculations [7]. The change in the equilibrium torsional angle of the 3s state with respect to the planar ground state is responsible for an activity in the ν_4 torsional mode (a_u) which had been noticed already in the first absorption analysis by Wilkinson and Mulliken [5].

Table 1 presents the different normal modes of ethylene, together with their corresponding frequencies, in the neutral ground state, in the 3s state and in the cation ground state. Both the D₂ and D_{2h} symmetry labels are reported in this table for the different modes. As pointed out in paragraph 3.1 above, D_{2h} symmetry group is pertinent for transitions towards Rydberg states from the neutral ground state, and it rules out excitation of odd quanta of ν_4 in the Rydberg states. The corresponding vibrational levels do not appear indeed in the REMPI spectra as shown below.

[insert table 2 about here]

Table 2 recalls the calculated geometrical parameters of the 3s state as compared with the neutral ground state and the cation ground state. Upon excitation of the π (1b_{3u}) valence orbital to the 3s Rydberg orbital, a lengthening of the C=C bond occurs from

1
2 the ground state to the $3s$ state [7], in good agreement with the experimental value [33].
3
4 In the cation, the C=C bond length has been calculated [37] to 1.4004 Å, close to that of
5
6 the $3s$ state. Excitation of the π orbital to the $3s$ orbital results in a twisted geometry as
7
8 said above. As shown in Table 2 the equilibrium torsion angles are very close in the $3s$
9
10 state [7] and in the cation ground state [37]. On what concerns the HCH scissor angle, it
11
12 is larger in the $3s$ Rydberg state than in the neutral ground state, and even larger than in
13
14 the cation ground state. From these values (see Table 2), the expected main contribution
15
16 to the REMPI spectrum should consist of excitation to totally symmetric vibronic levels
17
18 of the $3s$ state involving even quanta of the ν_4 torsion mode, and progressions in the ν_2
19
20 CC stretching mode and finally in the ν_3 CH₂ scissor mode.
21
22
23
24
25
26
27

28 3.3.1. Vibrational assignment

29
30 [insert figure 2 about here]

31
32
33 Figure 2 displays the (3+2) photon REMPI spectrum in the region of the $3s$ state. As
34
35 expected from the very short lifetime of the $\pi\pi^*$ V state, the observed features in the
36
37 energy range covered by Fig. 2 belong exclusively to the Rydberg transitions. Like in
38
39 the absorption spectrum [33] and as expected from the geometry changes described
40
41 above, the vibrational structure is dominated by progressions in $m\nu_2$ and $m\nu_2+2\nu_4$, but
42
43 surprisingly not by ν_3 bands. Note that the intensity of the vibrational transitions of Fig.
44
45 2 has not been corrected by the laser dye intensity. It is remarkable though that the
46
47 relative vibrational intensities and bandwidths match very well those of the absorption
48
49 spectrum, as shown in Fig. 1.
50
51
52
53

54
55 As was proposed earlier by Wilkinson and Mulliken [5] (see also page 534 of Ref.
56
57 [38]), and by Merer and Schoonveld [35], from the absorption spectrum analysis, a
58
59 progression in $m\nu_2+4\nu_4$ appears in the REMPI spectra as barely resolved shoulders lying
60
on the red side of the $(m+1)\nu_2$ bands. Our determination of $4\nu_4$ reported in Table 1 is in

1
2 good agreement with the value proposed by Ref. [35]. Table 3 summarizes all the
3
4 present three-photon assignments.
5

6 [insert table 3 about here]
7

8
9 At this point, it is interesting to take advantage of the absence of the underlying
10 V-N broad bands, for searching much weaker vibrational transitions in the $3s$ (3+2)
11 REMPI spectrum. In particular, the observation of the ν_3 CH₂ scissor vibration has been
12 recently proposed in the (2+1) REMPI spectrum of C₂H₄ by Rijkenberg and Buma [29]
13 through the observation of a two-photon symmetry allowed combination band $\nu_4+\nu_3$
14 leading to an estimated value of ν_3 of 1146 cm⁻¹ for C₂H₄. The search for three-photon
15 allowed bands involving the ν_3 mode in our spectrum results in a possible $m\nu_2+\nu_3$
16 progression shown in the spectrum of Fig. 2 with a ν_3 frequency value, given in Table 1,
17 close to the value proposed from the two-photon spectrum [29]. Unfortunately, these
18 bands are almost completely overlapped by the $m\nu_2+4\nu_4$ bands, which makes the ν_3
19 assignment only tentative at this stage of the analysis.
20
21
22
23
24
25
26
27
28
29
30
31
32
33
34

35
36 A more detailed comparison between our (3+2) REMPI data and the (2+1)
37 REMPI data obtained by Rijkenberg and Buma [29] on the $3s$ state, reveals a
38 discrepancy between the ν_2 frequency derived from their two-photon spectra analysis
39 and the ν_2 frequency measured either in the present (3+2) REMPI spectrum or in the
40 one-photon absorption spectrum [14]: from the assignment of the $\nu_2+\nu_4$ combination
41 band, Rijkenberg and Buma [29] extracted a ν_2 frequency of 1525 cm⁻¹, by far too large
42 as compared to the previous value of 1380 cm⁻¹ found by Wilkinson and Mulliken [5],
43 or by McDiarmid [14], or by the present work. This discrepancy can be corrected by
44 proposing two re-assignments of the (2+1) REMPI spectra of C₂H₄ and C₂D₄ in Ref.
45 [29]:
46
47
48
49
50
51
52
53
54
55
56
57
58
59
60

The first one consists of exchanging the assignments of the $\nu_2+\nu_4$ band and $5\nu_4$
band in C₂H₄. One convincing argument for exchanging these assignments is the

1
2 comparison between the vibrational spacing observed in the (2+1) REMPI-PES spectra
3 of Ref. [29], recorded from the above cited two-photon bands, and the corresponding
4 spacing measured with a better accuracy in the ZEKE spectrum of Ref. [32]. This
5 reassignment of the (2+1) photon spectra leads to a ν_2 value in the $3s$ state of C_2H_4 of
6 1336 cm^{-1} , and to a ν_2^+ value in the ground state of the $C_2H_4^+$ cation of 1480 cm^{-1} , in
7 better agreement with the previously measured $3s$ frequency [33], and with the more
8 recent cation frequency [32], respectively.

9
10 The above re-assignment of the two-photon bands in C_2H_4 implies a second re-
11 assignment of the $3s$ two-photon bands of C_2D_4 in Ref. [29], in order to keep a
12 consistent isotopic ratio between the C_2H_4 and C_2D_4 mode frequencies for the $5\nu_4$
13 bands. This can be done by exchanging the assignments of the $\nu_3+\nu_4$ and $5\nu_4$ bands in
14 the two-photon spectrum of C_2D_4 , in Ref. [29]. Again, these new assignment in C_2D_4
15 brings vibrational spacings in the cation, measured from the corresponding PES spectra
16 of Ref. [29], i.e. $5\nu_4^+ \approx 1000\text{ cm}^{-1}$ in better agreement with the ZEKE values of Ref.
17 [32], that is 982 cm^{-1} . In addition, these new assignments reasonably match the expected
18 isotopic ratio for the ν_3 frequency in the $3s$ state (i.e. 0.76).

3.3.2 Occurrence of (4+1) REMPI features embedded in the (3+2) REMPI spectra

19
20 Apart from the tentatively assigned combination bands involving ν_3 , other weaker
21 structures appear in Fig. 2. Some of these observed structures are reminiscent of (4+1)
22 REMPI nf transitions. The assignments proposed in Table 3, and displayed in Figure 2,
23 are supported by the previous observation of nf Rydberg states in the (2+1) photon
24 REMPI spectra of C_2H_4 and C_2D_4 [28]. Indeed, possible (4+1) resonances, reported in
25 Table 3, may occur superimposed on the (3+2) REMPI spectrum. Therefore an energy
26 scale for the four-photon energy is given at the top of Figure 2 and corresponds to the
27 region of the $4f$ and $5f$ complexes. The nf complexes have been analysed via two-photon
28
29
30
31
32
33
34
35
36
37
38
39
40
41
42
43
44
45
46
47
48
49
50
51
52
53
54
55
56
57
58
59
60

1 spectroscopy by Williams and Cool [28] ($n = 7-13$ for C_2H_4 and $n = 4-17$ for C_2D_4). They
2 essentially consist of two electronic components named by these authors as f_I and f_{II} ,
3 and exhibit mainly excitation in $2\nu_4$. The observed positions in Figure 2 match very well
4 the expected positions in C_2H_4 derived by applying the pertinent isotopic shift for origin
5 bands and excited vibrational bands, extracted from Ref. [28].
6
7
8
9
10
11
12

13
14 The non penetrating nf states are expected to be unperturbed and to mimic the
15 ionic ground state vibrational structure. The $2\nu_4$ and ν_2 frequencies derived from the
16 present (4+1) photon analysis of Table 3 are in agreement with the frequencies
17 previously derived from the two-photon analysis, and are very close indeed to the ion
18 frequencies given by Willitsch *et al.* [32]. More importantly, the observation of the very
19 weak nf transitions demonstrates that the REMPI spectrum displayed in Fig. 2 is, by far,
20 dominated by (3+2) processes in the 57000-63000 cm^{-1} region. Four-photon resonances
21 remain a minor process in this region and therefore should not contaminate the
22 photoelectron spectra recorded in the same region and shown in paragraph 3.3.4.
23
24
25
26
27
28
29
30
31
32
33
34

35 Another point concerns the weak feature at 79515 cm^{-1} (four-photon energy): it
36 is assigned to the $4f_I 3^1 4^2$ band by assuming a $\nu_3+2\nu_4$ band frequency identical to that
37 of the cation [32]. Note that in the C_2D_4 isotopomer, this vibrational band has also been
38 observed for the $4f_I$ state [28]. The ν_3 frequency of the $4f$ Rydberg states is very close to
39 that of the cation ground state, and finally is also in agreement with the two-photon
40 assignment of Ref. [28].
41
42
43
44
45
46
47
48
49
50
51
52

53 3.3.3 Summary on the ν_2 vibration frequency of the $3s$ state

54 It is interesting to compare the vibrational band intensities in the $3s$ transitions with that
55 of the PES spectrum recorded by Holland *et al.* [39]. This photoelectron spectrum
56 shows weaker ν_2 progressions as compared to strong ν_3 progressions. These intensities
57 have been explained by a Duschinsky rotation occurring in the transition from the
58
59
60

1
2 neutral ground state to the cation ground state, favouring the observation of ν_3 with
3
4 respect to ν_2 . Note that the corresponding PES spectrum [39] of C_2D_4 shows on the
5
6 other hand a dominant intensity of the ν_2 progressions as compared to the ν_3 bands,
7
8 corresponding to a different Duschinsky matrix in this isotopomer. The PFI-ZEKE
9
10 spectrum of Willitsch *et al.* [32] exhibits with very high rotational resolution a similar
11
12 trend favouring the ν_3 and $\nu_3+2\nu_4$ bands with respect to the ν_2 and $\nu_2+2\nu_4$ bands in
13
14 $C_2H_4^+$, and the reverse trend for $C_2D_4^+$. This situation has already been confirmed by
15
16 Rijkenberg and Buma [29] who calculated the Franck-Condon factors and Duschinsky
17
18 matrix upon ionisation of C_2H_4 and C_2D_4 . Excitation from the neutral ground state to the
19
20 $3s$ state shows very weak Franck-Condon factors involving the ν_3 scissor mode in our
21
22 REMPI spectra as well as in the absorption spectrum, indicating a different situation as
23
24 compared to excitation towards the cation ground state. Given the similar geometries
25
26 between the $3s$ state and the cation ground state (see Table 2), these Franck-Condon
27
28 factors are still unexplained.
29
30
31
32
33
34
35

36 A general comment can be drawn by comparing the measured vibrational
37
38 frequencies reported in Table 1. As expected from a Rydberg state, the observed $3s$
39
40 frequencies are much closer to the cation ground state frequencies than to the neutral
41
42 ground state value. Nevertheless, the ν_2 CC stretching frequency is significantly lower
43
44 in the $3s$ state than in the cation ground state, which is rather surprising given the almost
45
46 equal CC bond lengths in both states (see Table 2). This intriguing point has never been
47
48 commented to our knowledge, neither by spectroscopists nor by theoreticians. One
49
50 would expect the CC bond to be weaker in the cation than in the $3s$ Rydberg state.
51
52 Indeed, this lowest Rydberg orbital is expected to be rather penetrating and to
53
54 participate to some extent to the stability of the molecule. If the lower ν_2 frequency
55
56 value is to be correlated with a weakening of the CC bond in the $3s$ state (although this
57
58 correlation does not seem to be obvious from the computed equilibrium geometries of
59
60

1
2 Table 2), it could therefore reveal a slightly antibonding character of the $3s$ orbital. This
3
4 would deserve a more thorough analysis in terms of computed molecular orbitals.
5
6
7

8 9 3.3.4 Rydberg character of the $3s$ state: Photoelectron spectra

10
11 [insert Figure 3 about here]
12

13
14 The deviation from the Rydberg character of the $3s$ state can be better analysed through
15
16 the PES spectra. Three (3+2) REMPI-PES spectra have been recorded in the $3s$ region
17
18 and are presented in Figure 3. They correspond to ionisation from the $3s$ origin (panel
19
20 a), from the $3s4^2$ level (panel b) and from the $3s2^1$ level (panel c). Although the
21
22 vibrational structure of the cation is barely resolved, assignments are still possible from
23
24 these spectra. The strongest peaks around the zero ion internal energy correspond to the
25
26 expected $\Delta v_i=0$ propensity rule for a Rydberg state. In addition, significant ionisation to
27
28 mv_2^+ , v_3^+ and $mv_2^++2v_4^+$ also occurs, indicating a deviation from a pure Rydberg
29
30 character. The PES signal deteriorates with increasing energy; hence no assignment was
31
32 attempted for the highest energy features in Figs (3b) and (3c). The peaks around the
33
34 zero ion internal energy are expected to show a comparable resolution in the three
35
36 panels of Fig. 3. Thus, the increasing broadening from panel (a) to panel (c) has been
37
38 interpreted as unresolved and overlapping vibrational peaks, tentatively assigned in Figs
39
40 3 by reporting the accurate cation frequencies of Ref. [32] in dashed lines. The observed
41
42 vibrational activity in the PES spectrum can be understood in terms of non pure
43
44 Rydberg state, which is rather common for the lowest $3s$ Rydberg state of such
45
46 molecules. If one now compares the present PES spectra with those obtained by
47
48 Rijkenberg and Buma [29] in the (2+1) ionisation via the $3s4^3$ level, with a much better
49
50 resolution in their case, a striking difference is observed: in Ref. [29], only one
51
52 prominent photoelectron peak shows up at the $3v_4^+$ frequency of the ion, so that the
53
54 authors concluded to a predominant Rydberg character for the $3s$ Rydberg state of
55
56
57
58
59
60

1
2 ethylene. Two reasons can be proposed to explain this very surprising different
3
4 behaviour of the 3s state in our PES spectra:
5

6
7 - our (3+2) REMPI-PES spectrum may be contaminated by a quasi resonant state at the
8
9 fourth photon energy: this hypothesis is very unlikely, since we have shown in section
10
11 3.3.2 that the $4f$ and $5f$ states lying at the four-photon energy bring a very weak
12
13 contribution to the REMPI spectrum of Figure 2, and therefore should not contribute to
14
15 strong features in the PES spectrum.
16
17

18
19 - the (2+1) REMPI-PES experiment of Ref. [29] probes vibronic intermediate levels of
20
21 *gerade* symmetry in the D_{2h} group, while our experiment probes *ungerade* vibronic
22
23 intermediate levels, as said in section 3.1. Thus everything behaves as if the 3s
24
25 vibrational levels of *g* symmetry conformed to an almost pure Rydberg character, while
26
27 those of *u* symmetry (including the vibrationless level) behaved as less pure Rydberg
28
29 levels. A Rydberg-valence or a Rydberg-Rydberg vibronic coupling mediated by one
30
31 active mode might be invoked, as in the theoretical work of Mebel *et al.* [21]. For
32
33 instance these authors calculated a weak vibronic coupling between the 3s Rydberg state
34
35 and the N ground state by the ν_{12} (b_{3u} CH₂ wag) mode, leading to possible internal
36
37 conversion of this Rydberg state towards the ground state. This vibronically induced
38
39 internal conversion could explain the broadening observed in all *ungerade* bands of the
40
41 3s transition, both in absorption [33] and in the present REMPI experiment. A
42
43 substantial vibronic coupling between the $3p_y$ and 3s states, via the ν_8 (b_{2u}) and ν_9 (b_{2u})
44
45 modes, was also predicted in the same work [21]. On the other hand, Rijkenberg and
46
47 Buma [29] concluded to a negligible Rydberg-Rydberg coupling between the *gerade*
48
49 vibronic levels of the 3s and the $3p$ Rydberg states from their PES spectra. This could
50
51 be rationalized again in term of *g-u* “strong propensity rules” for vibronic couplings.
52
53
54
55
56
57

58
59 As a last remark, ν_3^+ and $\nu_3^+ + 2\nu_4^+$ cation vibrations have been tentatively assigned in
60
the spectra of Fig.3 in order to better fit the peak position at 156 meV in panel (a) and

1
2 the broad prominent peak around 200 meV in panel (c). These assignments need to be
3
4 confirmed by better resolved PES spectra, but they seem to indicate some activity in v_3
5
6 upon ionisation from the $3s$ state whereas such activity does not show up upon
7
8 excitation from the neutral ground state to the $3s$ state.
9
10

11 12 13 14 **3.4 The ns - nd Rydberg transition studied via (3+1) photon ionisation**

15
16 [insert Figure 4 about here]
17

18
19 Figure 4 presents the (3+1) REMPI spectrum of ethylene in the 68000 - 82000 cm^{-1}
20
21 energy region. All assignments are reported in Table 4. It is noticeable that the relative
22
23 intensities in the REMPI spectra of this spectral region are quite different from the ones
24
25 observed in the absorption spectrum (see Fig. 1a), although the peak positions match
26
27 quite well. Some of the bands disappear in the REMPI spectrum or become less intense
28
29 and there is no more obvious regularity in the vibrational structure. The prominence of
30
31 the v_2 and v_2+2v_4 bands observed in the $3s$ transition is no longer observable in the
32
33 higher ns - nd series.
34
35
36

37
38 [insert table 4 about here]
39

40
41 Although our REMPI spectra have been recorded with a much better resolution
42
43 than the absorption spectrum recorded by McDiarmid [14], a similar trend is observed
44
45 in the band broadenings of the one-photon and three-photon spectra. The region of the
46
47 $3d\sigma$ and $3d\delta$ transitions in Fig. 4 exhibits band broadenings similar to the region of the
48
49 $3s$ state studied above (see also Fig. 1). At higher energy, the $4s$ and $4d$ series appear
50
51 with a much broader profile in Fig. 4. Finally for the $5s$ and $5d$ series, the bands present
52
53 a narrower profile though in this high energy region spectral congestion leads to a more
54
55 complicated structure.
56
57
58
59
60

3.4.1. Origin bands

1
2 All origin bands established by McDiarmid from isotopomer analysis [14] are observed
3
4 in the (3+1) REMPI spectra, except for the $4d\delta$ member. At the expected energy of this
5
6 transition, i.e. 77604 cm^{-1} according to Ref. [14], no clear feature shows up in our
7
8 REMPI spectrum. Surprisingly, at slightly higher energy (77795 cm^{-1}), a rather intense
9
10 band could not be assigned in the present work. A careful look at the absorption spectra
11
12 [14] of the different isotopomers indicates the presence of this feature, albeit much
13
14 weaker. This feature has not been assigned so far and cannot be associated with a
15
16 member of a Rydberg series, neither corresponding to an origin band nor to a
17
18 vibrational band.
19
20
21
22

23
24 On the other hand, three new members of the $nd\pi_y$ series have been tentatively
25
26 assigned. The first member, $3d\pi_y$, is located at 66497 cm^{-1} and appears as a very weak
27
28 feature in the REMPI spectrum of Figure 1, indicated by an arrow on panel b). We
29
30 propose here a possible assignment as the $3d\pi_y$ Rydberg state of 1A_u symmetry,
31
32 forbidden by one-photon absorption but allowed by three-photon excitation as indicated
33
34 in Table 5. The corresponding quantum defect of 0.55 (see Table 5), indicative of a
35
36 penetrating orbital, can be rationalized by an occupied precursor orbital in the core for
37
38 this b_{3g} Rydberg orbital, as defined by Mulliken [40]. Further support of our assignment
39
40 is provided by the observation of the $4d\pi_y$ and $5d\pi_y$ features at 75551 and 79165 cm^{-1} ,
41
42 respectively, with identical quantum defect values (see Table 5). Note that a very weak
43
44 feature appeared in the absorption spectrum and was tentatively assigned by McDiarmid
45
46 to a $3p$ forbidden transition, on the basis of the quantum defect value of about 0.5 [14].
47
48
49
50
51
52
53
54

55 3.4.2. Excited vibrational bands

56
57 [insert table 5 about here]
58

59
60 Vibrational bands accompanying the above Rydberg band origins are assigned on the
spectrum of Fig. 4 and reported in Table 4. For comparison, the absorption vibrational

1
2 assignments given by McDiarmid [14] are also reported in this table. These REMPI
3
4 assignments complete the vibrational structure of the Rydberg series, in particular
5
6 through newly assigned ν_3 bands in the $4d\sigma$, $4s$, $5d\sigma$ and $5d\delta$ transitions. A summary of
7
8 the frequencies measured in the present work, namely ν_2 , ν_3 and $2\nu_4$, is presented in
9
10 Table 5, together with the frequency values of Ref. [14], in parenthesis, and with the
11
12 electronic origin energies and quantum defects of the observed ns and nd series. When n
13
14 increases from 3 to 5, the three mode frequencies get closer to the cation $C_2H_4^+$ values
15
16 [32], with the exception of the ν_2 frequency for the $4s$ and $5d\sigma$ members, anomalously
17
18 low as compared to the cation value. The $5s$ state, in particular, behaves as a pure
19
20 Rydberg state, with vibrational frequencies very close to that of the cation. Note that the
21
22 spectral features associated to the $5s$ bands shown in Fig. 4 are the narrowest in the
23
24 whole explored range, probably less affected by Rydberg-valence mixing or by internal
25
26 conversion than the other members of the observed series. A recent calculation of the
27
28 Rydberg series of ethylene lead to the conclusion that Rydberg states other than the $^1B_{1u}$
29
30 symmetry are pure Rydberg states [41]. This conclusion should nonetheless be
31
32 tempered, on the basis of the irregular broadening observed in the $n = 4$ to 5 Rydberg
33
34 series, as well as because of the absence of the $4d\delta$ states in the REMPI spectrum of
35
36 Fig. 4. Similar vibronic couplings as the ones invoked for the $3s$ state could possibly
37
38 occur between Rydberg states or between Rydberg states and the N ground state with
39
40 subsequent internal conversion competing with ionisation and affecting both the REMPI
41
42 bandwidths and band intensities.

3.4.3. Rydberg character of the $3d\sigma$ state: Photoelectron spectra

[insert Figure 5 about here]

Three (3+1) REMPI-PES spectra have been recorded in the $3d\sigma$ region and are presented in Figure 5. They correspond to ionisation from the $3d\sigma$ origin (panel a), from

1
2 the $3d\sigma 4^2$ level (panel b) and from the $3d\sigma 2^1$ level (panel c). These PES spectra have
3
4 been recorded with a resolution comparable to that of the $3s$ PES spectra of Fig. 3.
5
6

7 It is interesting to compare the two PES plots of Fig. 3 and Fig. 5. Like in the $3s$
8
9 levels, the $3d\sigma$ PES spectra reveal a vibrational activity upon ionisation, including the
10
11 ν_2^+ and $2\nu_4^+$ modes, but no clear activity appears in the ν_3^+ mode. This absence of ν_3^+
12
13 activity is expected from the very close frequency value of the $3d\sigma$ state and the cation
14
15 ground state (see Table 1 and Table 5). In the case of the $3d\sigma$ state, the ionisation step
16
17 only requires one-photon absorption from the intermediate level, as can be seen in Fig.
18
19 1, hence the PES spectra must reflect the Franck-Condon factors between the
20
21 $3d\sigma$ Rydberg state and the cation ground state. The similarity in the vibrational
22
23 progression for the PES spectra via the two Rydberg states $3s$ and $3d\sigma$, both of $^1B_{3u}$
24
25 symmetry, both penetrating states (quantum defects of 1.00 and 0.32, respectively),
26
27 seems to confirm the non-Rydberg character of the *ungerade* vibrational levels of the $3s$
28
29 state. Table 5 shows that the $2\nu_4$ frequencies of the $3s$ and $3d\sigma$ states are very close, 507
30
31 cm^{-1} and 515 cm^{-1} , respectively, but larger than the $2\nu_4^+$ cation frequency of 438 cm^{-1}
32
33 (Table 1). The PES's of Fig. 3 and Fig. 5 show indeed a similar activity in $2\nu_4^+$. As for
34
35 the ν_2 frequencies, the $3d\sigma$ state value is in between the $3s$ state value and the cation
36
37 value, as shown in Table 5 and Table 1. Appropriately, the ν_2^+ PES vibrational peaks
38
39 show up with less intensity for the $3d\sigma$ state (Fig. 5) than for the $3s$ state (Fig. 3). These
40
41 PES spectra lead therefore to a more qualified conclusion than that of the recent *ab*
42
43 *initio* calculations of Yamamoto *et al.* [41] who predicted a pure Rydberg character for
44
45 these Rydberg states.
46
47
48
49
50
51
52
53
54
55
56
57

58 4. CONCLUDING REMARKS

59 The analysis of the three-photon REMPI spectra of C_2H_4 has confirmed the earlier
60 vibrational assignment of the absorption spectrum by Merer and Shoonveld [33] and by

1
2
3
4
5
6
7
8
9
10
11
12
13
14
15
16
17
18
19
20
21
22
23
24
25
26
27
28
29
30
31
32
33
34
35
36
37
38
39
40
41
42
43
44
45
46
47
48
49
50
51
52
53
54
55
56
57
58
59
60

McDiarmid [14]. The absence of the $V \leftarrow N$ transition in these REMPI spectra has allowed to search for weaker Rydberg vibrational band structures, and to observe new bands involving the ν_3 mode in the $3s$ system, as well as new electronic components of the $3d$ complexes, i.e. the $3d\pi_y$, $4d\pi_y$ and $5d\pi_y$ components, forbidden by one-photon selection rules.

The vibrational ν_2 and $2\nu_4$ frequencies as well as the PES spectra from the lowest *ungerade* vibrational levels of the $3s$ state indicate a deviation from a pure Rydberg character, in contrast with the results obtained earlier by (2+1) REMPI-PES on the *gerade* vibrational levels of the same $3s$ Rydberg state. The same trend, although less pronounced, is observed for the $3d\sigma$ state.

Finally, most of the ns and nd Rydberg states observed in the present work present a strongly vibrationally dependent behaviour towards ionisation, as can be noted from the relative REMPI band intensities strongly varying with respect to the corresponding absorption features, even in a narrow energy range for which the laser intensity is almost constant. In addition, large variations in band broadening are observed between 57000 and 82000 cm^{-1} . All these observations support the hypothesis of vibronic couplings, either Rydberg-Rydberg or Rydberg-valence couplings, mediated by non-totally symmetric normal modes. Accurate and complete calculations of these non-adiabatic couplings still remain to be done in order to really explain the very complex VUV spectrum of ethylene.

On the other hand, the experimental task should also be pursued, in order to bring more precise experimental evidences of these vibronic couplings. Further work involving REMPI-PES via all the three-photon accessible ns and nd states ($n=3-6$) for both C_2H_4 and C_2D_4 isotopomers is needed in order to clarify the degree of Rydberg character, or conversely the strength of non-adiabatic couplings affecting these low lying Rydberg states of ethylene.

ACKNOWLEDGMENTS

First of all, two of the authors (D. G. and A.-L. R.) are most grateful to Dr. Ch. Jungen for having shared with them part of his thorough understanding of molecular Rydberg states.

The authors wish to thank Dr S. Douin and Dr T. Pino for their help in the earlier experimental stage. They acknowledge financial support from the “Programme de Physique et Chimie du Milieu Interstellaire” and from the “Programme National de Planétologie” (CNRS). One of the authors (K. A.) acknowledges financial support from the Atomic Energy Commission of Syria.

REFERENCES

- [1] A.J. Merer, R.S. Mulliken. *Chem. Rev.*, **69**, 639 (1969)
- [2] M.B. Robin, *Higher Excited states of Polyatomic Molecules, Vol II*, p. 4, Academic Press, New York, (1975).
- [3] R. McDiarmid. *On the electronic Spectra of Small Linear Polyenes*, p. 177, John Wiley & Sons. Inc. (1999).
- [4] R.S. Mulliken. *Phys. Rev.*, **43**, 279 (1933)
- [5] P.G. Wilkinson, R.S. Mulliken. *J. Chem. Phys.*, **23**, 1895 (1955)
- [6] R. McDiarmid, E. Charney. *J. Chem. Phys.*, **47**, 1517 (1967)
- [7] A.M. Mebel, Y.-T. Chen, S.-H. Lin. *J. Chem. Phys.*, **105**, 9007 (1996)
- [8] A.M. Mebel, M. Hayashi, K.K. Liang, S.H. Lin. *J. Phys. Chem.*, **103**, 10674 (1999)
- [9] M. Ben-Nun, T.J. Martinez. *J. Phys. Chem.*, **103**, 10517 (1999)
- [10] A. Hazra, H.H. Chang, M. Nooijen. *J. Chem. Phys.*, **121**, 2125 (2004)
- [11] R. Borrelli, A. Peluso. *J. Chem. Phys.*, **125**, 194308 (2006)
- [12] P. Farmanara, V. Stert, W. Radloff. *Chem. Phys. Lett.*, **288**, 518 (1998)
- [13] J.M. Mestdagh, J.P. Visticot, M. Elhanine, B. Soep. *J. Chem. Phys.*, **113**, 237 (2000)
- [14] R. McDiarmid. *J. Phys. Chem.*, **84**, 64 (1980)
- [15] R.J. Buenker, S.D. Peyerimhoff. *Chem. Phys. Lett.*, **36**, 415 (1975)
- [16] R.S. Mulliken. *Chem. Phys. Lett.*, **46**, 197 (1977)
- [17] K.B. Wiberg, C.M. Hadad, J.B. Foresman, W.A. Chupka. *J. Phys. Chem.*, **96**, 10756 (1992)
- [18] C. Petrongolo, R.J. Buenker, S.D. Peyerimhoff. *J. Chem. Phys.*, **76**, 3655 (1982)
- [19] C. Petrongolo, R.J. Buenker, S.D. Peyerimhoff. *J. Chem. Phys.*, **78**, 7284 (1983)
- [20] W. Siebrand, F. Zerbetto, M.Z. Zgierski. *Chem. Phys. Lett.*, **174**, 119 (1990)

- 1
2
3
4
5
6
7
8
9
10
11
12
13
14
15
16
17
18
19
20
21
22
23
24
25
26
27
28
29
30
31
32
33
34
35
36
37
38
39
40
41
42
43
44
45
46
47
48
49
50
51
52
53
54
55
56
57
58
59
60
- [21] A.M. Mebel, M. Hayashi, S.H. Lin. *Chem. Phys.Lett.*, **274**, 281 (1997)
- [22] M. Ben-Nun, T.J. Martinez. *Chem. Phys.*, **259**, 237 (2000)
- [23] K.K. Baeck, T.J. Martinez. *Chem. Phys.Lett.*, **375**, 299 (2003)
- [24] M. Barbatti, J. Paier, H. Lischka. *J.Chem.Phys.*, **121**, 11614 (2004)
- [25] C. Jungen. *J. Chem. Phys.*, **53**, 4168 (1970)
- [26] V. Blanchet, S. Boyé, S. Zamith, A. Campos, B. Girard, J. Liévin, D. Gauyacq.
J. Chem. Phys., **119**, 3751 (2003)
- [27] A. Gedanken, N.A. Kuebler, M.B. Robin. *J. Chem. Phys.*, **76**, 46 (1982)
- [28] B.A. Williams, T.A. Cool. *J. Chem. Phys.*, **94**, 6358 (1991)
- [29] R.A. Rijkenberg, W.J. Buma. *J. Phys. Chem. A*, **106**, 3727 (2002)
- [30] S. Guizard, N. Shafizadeh, M. Horani, D. Gauyacq. *J. Chem. Phys.*, **94**, 7046
(1991)
- [31] K. Alnama, J.-H. Fillion, D. Gauyacq. *Journal of Quantitative Spectroscopy and
Radiative Transfer*, **105**, 139 (2007)
- [32] S. Willitsch, U. Hollenstein, F. Merkt. *J. Chem. Phys.*, **120**, 1761 (2004)
- [33] A.J. Merer, L. Schoonveld. *Can. J. Phys.*, **47**, 1731 (1969)
- [34] S. Boyé, A. Campos, J.H. Fillion, S. Douin, N. Shafizadeh, D. Gauyacq.
Compte-Rendu de Physique de l'Académie des Sciences, Paris, **5**, 239 (2004)
- [35] A.J. Merer, L. Schoonveld. *J. Chem. Phys.*, **48**, 522 (1968)
- [36] P.D. Foo, K.K. Innes. *J. Chem. Phys.*, **60**, 4582 (1974)
- [37] M.L. Abrams, E.F. Valeev, C.D. Sherrill, T.D. Crawford. *J. Phys. Chem. A*, **106**,
2671 (2002)
- [38] G. Herzberg. *Molecular Spectra and Molecular Structure; III Electronic spectra
and electronic structure of polyatomic molecules*, p. 534, Van Nostrand
Reinhold, New York (1966).

- 1
2 [39] D.M.P. Holland, D.A. Shaw, M.A. Hayes, L.G. Shpinkova, E.E. Rennie, L.
3
4 Karlsson, P. Baltzer, B. Wannberg. *Chem. Phys.*, **219**, 91 (1997)
5
6
7 [40] R.S. Mulliken. *J. Chem. Phys.*, **66**, 2448 (1977)
8
9 [41] S. Yamamoto, H. Tatewaki. *Chem. Phys.*, **295**, 47 (2003)
10
11 [42] R.J. Sension, B.S. Hudson. *J. Chem. Phys.*, **90**, 1377 (1989)
12
13 [43] J. Duncan, J.L. McKean, P.D. Mallinson. *J. Mol. Spectrosc.*, **45**, 221 (1973)
14
15 [44] X. Xing, M.-K. Bahng, P. Wang, K.-C. Lau, S.J. Baek, C.Y. Ng. *J. Chem. Phys.*,
16
17 **125**, 133304 (2006)
18
19
20
21
22
23
24
25
26
27
28
29
30
31
32
33
34
35
36
37
38
39
40
41
42
43
44
45
46
47
48
49
50
51
52
53
54
55
56
57
58
59
60

Table 1: Experimental vibrational frequencies of the \tilde{X} ground state, $3s$ Rydberg state and \tilde{X}^+ cation ground state of ethylene (in cm^{-1}). Within the symmetry conventions adopted here, the C=C bond is assigned as the z axis and the x axis is perpendicular to the plane of the ground state molecule (see for instance Ref. [42] for a discussion on the many conventions used to describe ethylene normal modes).

Normal mode	Description	D_{2h}	D_2	\tilde{X} ($N, {}^1A_g$) ^{a)}	$3s$ ($R, {}^1B_{3u}$)	\tilde{X}^+ ($D_0, {}^2B_{3u}$)
ν_1	CH s stretch	a_g	a	3026		
ν_2	C=C stretch	a_g	a	1630	1374 ^{b)} 1376 ^{d)}	1487.7 ^{c)} 1488.3 ^{e)}
ν_3	CH ₂ scissors	a_g	a	1342	1211 ^{d)}	1258.7 ^{c)}
ν_4	torsion	a_u	a	1023		83.7 ^{c)} 84.1 ^{e)}
$2\nu_4$					461 ^{b)} 490 ^{d)}	438.2 ^{c)}
$3\nu_4$						764.6 ^{c)}
$4\nu_4$					1153 ^{d)}	1162.1 ^{c)}
ν_5	CH a stretch	b_{1u}	b_1	3021		2978.7 ^{e)}
ν_6	CH ₂ scissors	b_{1u}	b_1	1444		1411.7 ^{e)}
ν_7	CH ₂ wag	b_{2g}	b_2	940		
ν_8	CH a stretch	b_{2u}	b_2	3105		
ν_9	CH ₂ rock	b_{2u}	b_2	826		
ν_{10}	CH stretch	b_{3g}	b_3	3103		
ν_{11}	CH ₂ rock	b_{3g}	b_3	1220		
ν_{12}	CH ₂ wag	b_{3u}	b_3	949		901.3 ^{c)}

a) taken from Ref. [43]

b) taken from Ref. [14]

c) taken from Ref. [32]

d) this work. The ν_2 value is taken from the 2^1_0 band; ν_3 , $2\nu_4$ and $4\nu_4$ are average values derived from the combination bands observed in Fig.2 (see Table 3)

e) taken from Ref. [44]

Table 2: Calculated equilibrium geometrical parameters for the neutral ground state (N, 1A_g), the $3s$ Rydberg state (R, $^1B_{3u}$) and the cation ground state (D_0 , $^2B_{3u}$) of C_2H_4 . Only the pertinent coordinates in relation with the observed vibrational structure are reported in the Table.

Parameter	\tilde{X}^a	$3s^a$	\tilde{X}^{+b}
$R_{C=C}$ [\AA]	1.338	1.402	1.4004
θ_{HCH} scissor [$^\circ$]	116.6	122.4	118.9
$\tau_{C=C}$ torsion [$^\circ$]	0	20	21

^{a)} Mebel *et al.* Ref. [7]

^{b)} Abrams *et al.* Ref. [37]

Table 3: Assignments for the different transitions observed by (3+2) or (4+1) REMPI spectroscopy of ethylene. The observed peak positions are given with $\pm 20 \text{ cm}^{-1}$ accuracy. Energies marked with an asterisk (*) are located on a peak shoulder. Parenthesis indicate the corresponding three-photon energy for a four-photon process.

Observed energy for a 3hv process (cm^{-1})	Observed energy for a 4hv process (cm^{-1})	Assignment (this work)		Ref. [5]
		3hv	4hv	
57333		$3s 0^0$		57336.0
57840		$3s 4^2$		57832.8
(58382)	77843		$4f_1 0^0$	
58490		$3s 4^4$		58420.0*
(58490)	77987		$4f_{11} 0^0$	
58520		$3s 3^1$		
(58696)	78261		$4f_1 4^2$	
58709		$3s 2^1$		58706.3
(58809)	78412*		$4f_{11} 4^2$	
59200		$3s 2^1 4^2$		59199.1
(59253)	79004*		$4f_1 4^4$	
(59324)	79096		$4f_1 3^1$	
(59450)	79267		$4f_1 2^1$	
(59636)	79515		$4f_1 3^1 4^2$	
59894		$3s 2^1 4^4$		59904.7*
59941		$3s 2^1 3^1$		
60057		$3s 2^2$		60055.4
(60242)	80323		$5f_1 0^0$	
(60345)	80460		$5f_{11} 0^0$	
60535		$3s 2^2 4^2$		60513.2
(60557)	80743		$5f_1 4^2$	
61207		$3s 2^2 4^4$		61226.0*
61270		$3s 2^2 3^1$		
61367		$3s 2^3$		61379.1
61849		$3s 2^3 4^2$		61838.6
62485*		$3s 2^3 4^4$		62547.0*
62580		$3s 2^3 3^1$		
62707		$3s 2^4$		62689.5

Table 4: Assignments for the different *ns-nd* series of ethylene observed by (3+1) REMPI spectroscopy. Transitions located on a shoulder are indicated by an asterisk (*).

Observed three-photon energy (cm ⁻¹)	Ref. [14]	Tentative assignment	Observed three- photon energy (cm ⁻¹)	Ref.[14]	Tentative assignment
68687		unassigned	76500	-	4s 2 ² 4 ²
69530	69531	3dσ 0 ⁰	76753	76728	4dσ 0 ⁰
70045	70033	3dσ 4 ²	77010	-	4dπ _y 2 ¹
70793*	70746	3dσ 3 ¹	77213	77204	4dσ 4 ²
70931	70887	3dσ 2 ¹	-	77604	4dδ 0 ⁰
71437	-	3dσ 2 ¹ 4 ²	77795		unassigned
71782	71813	3dδ 0 ⁰	77945	-	4dσ 3 ¹
71976	-	3dσ 2 ¹ 3 ¹	77945	77912	4dδ 4 ²
72150	72182	3dδ 4 ²	78155	-	4dσ 2 ¹
72355	-	3dσ 2 ²	78302	78302	5s 0 ⁰
72837	-	3dσ 2 ² 4 ²	78558		4dσ 2 ¹ 4 ²
73038	73025	3dδ 3 ¹	78741	78728	5s 4 ²
73260*	73228	3dδ 2 ¹	78985	78970	4dδ 2 ¹
73290*	-	4s 0 ⁰	79165	-	5dπ _y 0 ⁰
73552*		3dσ 2 ² 3 ¹	79553	-	4dσ 2 ²
73730	-	4s 4 ²	79553	79548	5s 3 ¹
73730	-	3dδ 2 ¹ 4 ²	79604		5dπ _y 4 ²
73730	-	3dσ 2 ³	79797	-	5dσ 0 ⁰
74282		3dσ 2 ³ 4 ²	79797	79796	5s 2 ¹

74434	-	$4s\ 3^1$	80227	80222	$5s\ 2^1 4^2$
74434	74440	$3d\delta\ 2^1 3^1$	80227	-	$5d\sigma\ 4^2$
74590	-	$4s\ 2^1$	80227	80218	$5d\delta\ 0^0$
74590	-	$3d\delta\ 2^2$	80423	-	$4d\delta\ 2^2$
74979	-	$3d\sigma\ 2^3\ 3^1$	80626	80632	$5d\delta\ 4^2$
75256	-	$3d\sigma\ 2^4$	81033	-	$5d\sigma\ 3^1$
75256	-	$3d\delta\ 2^2\ 4^2$	81186	-	$5d\sigma\ 2^1$
75551	-	$4d\pi_y\ 0^0$			
75815	-	$4s\ 2^1\ 3^1$	81186	-	$5s\ 2^2$
76100*	-	$4d\pi_y\ 4^2$	81472	-	$5d\delta\ 3^1$
76100*	-	$4s\ 2^2$	81733	-	$5d\sigma\ 2^1\ 4^2$
76500	-	$3d\delta\ 2^3\ 4^2$			

For Peer Review Only

Table 5: Quantum defects (δ) and observed vibrational level differences (in cm^{-1}) of ns and nd Rydberg states of C_2H_4 . δ is calculated by using the well-known Rydberg formula: $\delta = n - [\text{Ry}/(\text{IP} - E)]^{1/2}$ where n is the principal quantum number, $\text{Ry} = 109735 \text{ cm}^{-1}$, $\text{IP} = 84790.4 \text{ cm}^{-1}$ (Ref. [32]) and E is the origin band energy of the Rydberg state in cm^{-1} . Frequencies are reported within $\pm 30 \text{ cm}^{-1}$. Values in parenthesis are taken from Ref. [14]. The asterisk indicates transitions forbidden by one-photon absorption.

State	D_{2h} Symmetry	Energy 0^0_0	δ	2^1_0	3^1_0	4^2_0
$3s$	B_{3u}	57333	1.00	1376	1187	507
				(1374)		(461)
$4s$	B_{3u}	73290	0.91	1300	1144	440
$5s$	B_{3u}	78302	0.89	1495	1251	439
				(1494)	(1246)	(426)
$3d\sigma$	B_{3u}	69530	0.32	1401	1263	515
				(1356)	(1215)	(502)
$4d\sigma$	B_{3u}	76753	0.30	1402	1192	460
						(476)
$5d\sigma$	B_{3u}	79797	0.31	1389	1236	430
$3d\pi_y$	A_u^*	66497	0.55	-	-	-
$4d\pi_y$	A_u^*	75551	0.55	1459	-	549
$5d\pi_y$	A_u^*	79165	0.58	-	-	439
$3d\delta$	B_{2u}	71782	0.096	1478	1256	368
				(1415)	(1212)	(369)
$4d\delta$	B_{2u}	(77604)	-	1381	-	341
				(1366)	(1242)	(308)
$5d\delta$	B_{2u}	80227	0.096	-	1245	399
						(414)

FIGURE CAPTIONS

Figure 1: Survey of: (panel a) the one-photon absorption spectrum recorded in this work, (panel b) the three-photon REMPI spectrum of ethylene in the 56000-88000 cm^{-1} three-photon energy region, without any laser intensity corrections, and (panel c) the corresponding dye laser curves. Note that in the region below 63593 cm^{-1} , absorption of two photons is required for ionisation. Note also that in the (3+2) REMPI region, the $V \leftarrow N$ transition disappears from the REMPI signal, leaving only the vibrational structure of the $3s \leftarrow N$ system. The arrow displayed at 66497 cm^{-1} on panel (b) indicates the position of the $3d\pi_y$ origin band.

Figure 2: Region of the $3s$ Rydberg state probed by (3+2) REMPI spectroscopy in the range 56500-63000 cm^{-1} together with the vibrational assignments involving progressions in ν_2 , $\nu_2+2\nu_4$, $\nu_2+4\nu_4$ and $\nu_2+\nu_3$. The three-photon effective resolution of these scans is about 1 cm^{-1} . Note that the two scans used to cover the related spectral range of the spectrum (56500-61700 cm^{-1} and 59500-63000 cm^{-1}) have not been corrected from the laser intensity but have been approximately normalised to each other by overlapping of the $3s$ $2^2 4^2$ bands. Tentative assignments for nf Rydberg series observed by (4+1) REMPI spectroscopy are also reported on the spectrum with the corresponding four-photon energy scale at the top of the plot.

Figure 3: (3+2) REMPI-PES spectra of the $3s$ Rydberg state for: (a) the origin band at 57333 cm^{-1} , (b) the $2\nu_4$ vibrational band at 57840 cm^{-1} , and (c) the ν_2 vibrational band at 58709 cm^{-1} . The poor energy resolution (about 90 meV) is probably due to space charge effects occurring in the interaction volume, but a vibrational structure of the cation is still detectable in the three spectra. Note that at negative ion energy, two vibrational

1
2 peaks appear in the spectrum of panel (a) and can be associated with six-photon
3
4 ionisation [most probably (3+3)] into the \tilde{A} state of the $C_2H_4^+$ cation (origin band+first
5
6 vibrational level as given in Ref. [39]). The occurrence of prominent overlapping
7
8 vibrational PES peaks in the cation explains the increasing broadening of the principal
9
10 peak around zero ion internal energy from panel (a) to (c).
11
12
13
14

15
16 **Figure 4:** Region of the ns - nd Rydberg series probed by (3+1) REMPI spectroscopy in
17
18 the range 68000-82000 cm^{-1} . The vibrational assignments reported on the graph as a
19
20 triplet ($m n p$) corresponds to the combination bands $mv_2+nv_3+pv_4$. In addition,
21
22 tentative assignments for the $4d\pi_y$ and $5d\pi_y$ states are reported on the spectrum. Various
23
24 band broadenings are observed in these spectra, all recorded with the same three-photon
25
26 effective resolution of 1 cm^{-1} . The question mark indicates the expected position of the
27
28 unobserved $4d\delta$ band (at 77604 cm^{-1} according to Ref. [14]).
29
30
31
32
33
34
35

36 **Figure 5:** (3+1) REMPI-PES spectra of the $3d\sigma$ Rydberg state for: (a) the origin band at
37
38 69530 cm^{-1} , (b) the $2v_4$ vibrational band at 70045 cm^{-1} , and (c) the v_2 vibrational band at
39
40 70931 cm^{-1} . These three spectra exhibit a significant activity in the $2v_4^+$ mode as
41
42 compared to the v_2^+ and v_3^+ modes more prominent in the $3s$ PES spectra of Figs 3. The
43
44 energy resolution is similar to that of Fig. 3, i.e. 90 meV at best, in the zero ion energy
45
46 region.
47
48
49
50
51
52
53
54
55
56
57
58
59
60